(12) INTERNATIONAL APPLICATION PUBLISHED UNDER THE PATENT COOPERATION TREATY (PCT)

(19) World Intellectual Property Organization
International Bureau

(43) International Publication Date
30 June 2016 (30.06.2016)

WIPO | PCT

(10) International Publication Number
WO 2016/106286 A1

(51) International Patent Classification:
G01N 33/483 (2006.01) *G01N 33/50* (2006.01)
G01N 23/20 (2006.01) *G01N 33/566* (2006.01)

(21) International Application Number:
PCT/US2015/067285

(22) International Filing Date:
22 December 2015 (22.12.2015)

(25) Filing Language: English

(26) Publication Language: English

(30) Priority Data:
62/096,334 23 December 2014 (23.12.2014) US

(71) Applicant: **BIODESY, INC.** [US/US]; 384 Oyster Point Boulevard, #8, South San Francisco, CA 94080 (US).

(72) Inventor: **SALAFSKY, Joshua**; 188 Liberty Street, San Francisco, CA 94110 (US).

(74) Agents: **SUNDBERG, Steven A.** et al.; Wilson Sonsini Goodrich & Rosati, 650 Page Mill Road, Palo Alto, CA 94304-1050 (US).

(81) Designated States *(unless otherwise indicated, for every kind of national protection available)*: AE, AG, AL, AM, AO, AT, AU, AZ, BA, BB, BG, BH, BN, BR, BW, BY, BZ, CA, CH, CL, CN, CO, CR, CU, CZ, DE, DK, DM, DO, DZ, EC, EE, EG, ES, FI, GB, GD, GE, GH, GM, GT, HN, HR, HU, ID, IL, IN, IR, IS, JP, KE, KG, KN, KP, KR, KZ, LA, LC, LK, LR, LS, LU, LY, MA, MD, ME, MG, MK, MN, MW, MX, MY, MZ, NA, NG, NI, NO, NZ, OM, PA, PE, PG, PH, PL, PT, QA, RO, RS, RU, RW, SA, SC, SD, SE, SG, SK, SL, SM, ST, SV, SY, TH, TJ, TM, TN, TR, TT, TZ, UA, UG, US, UZ, VC, VN, ZA, ZM, ZW.

(84) Designated States *(unless otherwise indicated, for every kind of regional protection available)*: ARIPO (BW, GH, GM, KE, LR, LS, MW, MZ, NA, RW, SD, SL, ST, SZ, TZ, UG, ZM, ZW), Eurasian (AM, AZ, BY, KG, KZ, RU, TJ, TM), European (AL, AT, BE, BG, CH, CY, CZ, DE, DK, EE, ES, FI, FR, GB, GR, HR, HU, IE, IS, IT, LT, LU, LV, MC, MK, MT, NL, NO, PL, PT, RO, RS, SE, SI, SK, SM, TR), OAPI (BF, BJ, CF, CG, CI, CM, GA, GN, GQ, GW, KM, ML, MR, NE, SN, TD, TG).

Published:

— *with international search report (Art. 21(3))*

(54) Title: ATTACHMENT OF PROTEINS TO INTERFACES FOR USE IN NONLINEAR OPTICAL DETECTION

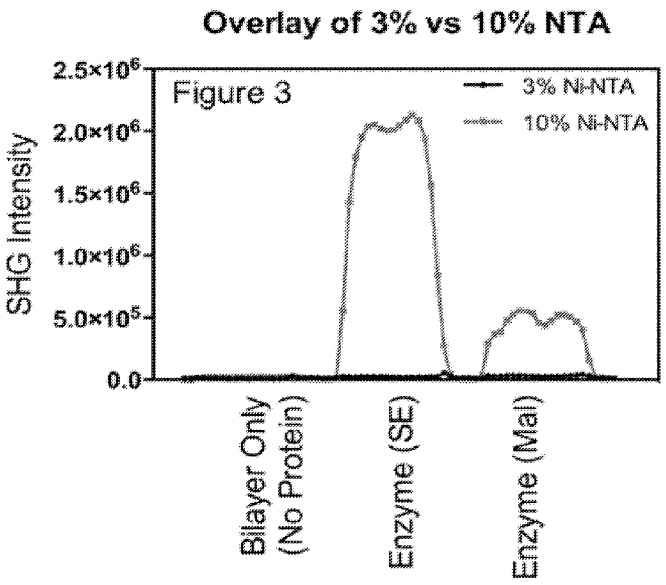

FIG. 4

(57) Abstract: Methods are disclosed for tethering a biological entity to a substrate comprising: (a) forming a supported lipid bilayer on a surface of a substrate, wherein the supported lipid bilayer comprises an anchor molecule conjugated to a first affinity tag that is present in the lipid bilayer at a concentration greater than or equal to 5 mole percent; and (b) contacting the supported lipid bilayer with a biological entity, wherein the biological entity comprises an nonlinear-active label and a second affinity tag capable of binding to the first affinity tag, thereby tethering the biological entity to the supported lipid bilayer in an oriented fashion.

WO 2016/106286 A1

ATTACHMENT OF PROTEINS TO INTERFACES FOR USE IN NONLINEAR OPTICAL DETECTION

CROSS-REFERENCE

[0001] This application claims the benefit of U.S. Provisional Application No. 62/096,334, filed December 23, 2014, which application is incorporated herein by reference in its entirety.

BACKGROUND

[0002] Second harmonic generation (SHG) is a nonlinear optical process which may be configured as a surface-selective detection technique that enables detection of conformational change in proteins and other biological targets (as described previously, for example, in U.S. Patent Nos. 6,953,694 and 8,497,703). In order to deploy SHG-based detection of conformational change in a convenient and high throughput format, it will be advantageous to design novel methods for immobilizing proteins on substrate surfaces, and novel mechanisms for rapid, precise, and interchangeable positioning of substrates (comprising the tethered biological targets to be analyzed) with respect to the optical system used to deliver excitation light, which ensure that both a high degree of orientation of the protein molecules at the optical interface and efficient optical coupling between the excitation light and the substrate surface are maintained.

[0003] The methods and compositions disclosed herein provide means for tethering or immobilizing protein molecules on optical interfaces in a manner that ensures both uniform surface coverage of the optical interface and a high degree of orientation of the molecules, thereby providing for significant enhancements of SHG and other nonlinear optical signals and improved signal-to-noise ratios.

SUMMARY

[0004] Disclosed herein are methods for tethering a biological entity to a substrate comprising: (a) forming a supported lipid bilayer on a surface of a substrate, wherein the supported lipid bilayer

[0005] comprises an anchor molecule that comprises or bears a first affinity tag that is present in the lipid bilayer at a concentration greater than or equal to 5 mole percent; and (b) contacting the supported lipid bilayer with a biological entity, wherein the biological entity comprises a nonlinear-active label and a second affinity tag capable of binding to the first affinity tag, thereby tethering the biological entity to the supported lipid bilayer in an oriented

fashion. In some aspects, the methods further comprise detecting a non-linear optical signal arising from the tethered biological entity.

[0006] In some aspects, the substrate is fabricated from a material selected from the group consisting of glass, fused-silica, a polymer, or any combination thereof. In some aspects, the first affinity and

[0007] second affinity tags are Ni-NTA and poly-histidine tags. In some aspects, the poly-histidine tag is attached to the N-terminus of a protein. In some aspects, the poly-histidine tag is attached to the C-terminus of a protein. In some aspects, the poly-histidine tag comprises between 4 and 24 histidine residues. In some aspects, the poly-histidine tag comprises 8 histidine residues. In some aspects, the poly-histidine tag comprises 6 histidine residues. In some aspects, the first affinity tag comprises Co-CMA and the second affinity tag comprises a poly-histidine tag. In some aspects, the first affinity tag comprises biotin and the second affinity tag comprises streptavidin. In some aspects, the first affinity tag comprises biotin and the second affinity tag comprises avidin. In some aspects, the first affinity tag comprises biotin and the second affinity tag comprises neutravidin. In some aspects, the non-linear optical signal is second harmonic light. In some aspects, the non-linear optical signal is sum frequency light. In some aspects, the non-linear optical signal is difference frequency light. In some aspects, the biological entity is selected from the group consisting of cells, proteins, peptides, receptors, enzymes, antibodies, DNA, RNA, biological molecules, oligonucleotides, small molecules, synthetic molecules, carbohydrates, or any combination thereof. In some aspects, the anchor molecule comprising the first affinity tag is adjusted to a value ranging from 5 mole percent to 100 mole percent of the lipid bilayer. In some aspects, the non-linear optical signal detected increases by at least 5x when the concentration of the anchor molecule comprising the first affinity tag is increased by a factor of 2x. In some aspects, the non-linear optical signal detected increases by at least 10x when the concentration of the anchor molecule comprising the first affinity tag is increased by a factor of 2x. In some aspects, the non-linear optical signal detected increases by at least 20x when the concentration of the anchor molecule comprising the first affinity tag is increased by a factor of 2x. In some aspects, the dependence of the non-linear optical signal on the concentration of the anchor molecule comprising the first affinity tag is described by a power law having an exponent greater than 2. In some aspects, the methods further comprise incubating the supported lipid bilayer with the biological entity for about 10 minutes to about 60 minutes. In some aspects, the biological entity is present at a concentration of about 0.1 uM to 10 uM. In some aspects, the supported lipid bilayer comprises 1,2-dioleoyl-sn-glycero-3-phosphocholine. In some

aspects, the anchor molecule conjugated to the first affinity tag comprises 1,2-dioleoyl-sn-glycero-3-[(N-(5-amino-1-carboxypentyl)iminodiacetic acid)succinyl] (nickel salt). In some aspects, the biological entity is a protein. In some aspects, the protein is present at a concentration of less than 2 uM. In some aspects, the amount of protein used is less than 500 ng.

[0008] Also disclosed herein are methods for detecting conformational change in a biological entity comprising: (a) illuminating a substrate with one or more light beams at one or more fundamental frequencies, wherein the substrate comprises a supported lipid bilayer, and wherein the supported lipid bilayer further comprises a Ni-NTA bearing lipid present at a concentration of greater than 5 mole percent, and wherein a biological entity comprising a non-linear active label and poly-histidine tag is tethered to the supported lipid bilayer; (b) measuring a non-linear optical signal arising from the tethered biological entity; (c) optionally contacting the tethered biological entity with one or more candidate binding partners; (d) optionally measuring a non-linear optical signal arising from the tethered biological entity in contact with the one or more candidate binding partners; and (e) optionally comparing the non-linear optical signals measured in steps (b) and (d) to detect a conformational change in the biological entity.

[0009] In some aspects, the substrate is fabricated from a material selected from the group consisting of glass, fused-silica, a polymer, or any combination thereof. In some aspects, the biological entity is a protein and the poly-histidine tag is attached to the N-terminus of the protein. In some aspects, the biological entity is a protein and the poly-histidine tag is attached to the C-terminus of the protein. In some aspects, the poly-histidine tag comprises between 4 and 24 histidine residues. In some aspects, the poly-histidine tag comprises 8 histidine residues. In some aspects, the polyhistidine tag comprises 6 histidine residues. In some aspects, the non-linear optical signal is second harmonic light. In some aspects, the non-linear optical signal is sum frequency light. In some aspects, the non-linear optical signal is difference frequency light. In some aspects, the supported lipid bilayer comprises 1,2-dioleoyl-sn-glycero-3-phosphocholine. In some aspects, the Ni-NTA bearing lipid comprises 1,2-dioleoyl-sn-glycero-3-[(N-(5-amino-1-carboxypentyl)iminodiacetic acid)succinyl] (nickel salt). In some aspects, the biological entity is selected from the group consisting of cells, proteins, peptides, receptors, enzymes, antibodies, DNA, RNA, biological molecules, oligonucleotides, small molecules, synthetic molecules, carbohydrates, or any combination thereof. In some aspects, the biological entity is a protein. In some aspects, the protein is

present at a concentration of less than 2 uM. In some aspects, the amount of protein used is less than 500 ng.

[0010] Disclosed herein are devices comprising: (a) a substrate, wherein the substrate further comprises a supported lipid bilayer; and (b) a biological entity, wherein the biological entity comprises a non-linear active label and is tethered to the supported lipid bilayer using a pair of affinity tags, and wherein one of the affinity tags is attached to the supported lipid bilayer by means of an anchor molecule that is present in the bilayer at a concentration of greater than or equal to 5 mole percent, and the other affinity tag is attached to the biological entity; wherein the device is capable of producing a non-linear optical signal when exposed to excitation light.

[0011] In some aspects, the substrate is fabricated from a material selected from the group consisting of glass, fused-silica, a polymer, or any combination thereof. In some aspects, one of the affinity tags comprises Ni-NTA and the other affinity tag comprises a poly-histidine tag. In some aspects, the poly-histidine tag is attached to the N-terminus of a protein. In some aspects, the poly-histidine tag is attached to the C-terminus of a protein. In some aspects, the poly-histidine tag comprises between 4 and 24 histidine residues. In some aspects, the poly-histidine tag comprises 8 histidine residues. In some aspects, the poly histidine tag comprises 6 histidine residues. In some aspects, one of the affinity tags comprises Co-CMA and the other affinity tag comprises a poly-histidine tag. In some aspects, one of the affinity tags comprises biotin and the other affinity tag comprises streptavidin. In some aspects, one of the affinity tags comprises biotin and the other affinity tag comprises avidin. In some aspects, one of the affinity tags comprises biotin and the other affinity tag comprises neutravidin. In some aspects, the non-linear optical signal is second harmonic light. In some aspects, the non-linear optical signal is sum frequency light. In some aspects, the non-linear optical signal is difference frequency light. In some aspects, the biological entity is selected from the group consisting of cells, proteins, peptides, receptors, enzymes, antibodies, DNA, RNA, biological molecules, oligonucleotides, small molecules, synthetic molecules, carbohydrates, or any combination thereof. In some aspects, the supported lipid bilayer comprises 1,2-dioleoyl-sn-glycero-3-phosphocholine. In some aspects, the anchor molecule bearing the first affinity tag comprises 1,2-dioleoyl-sn-glycero-3-[(N-(5-amino-1-carboxypentyl)iminodiacetic acid)succinyl] (nickel salt). In some aspects, the concentration of the anchor molecule bearing one of the affinity tag is adjusted to a value ranging from 5 mole percent to 100 mole percent.

[0012] Disclosed herein are kits comprising: (a) a device comprising a substrate; (b) a lipid suspension, wherein the lipid suspension is capable of forming a supported lipid bilayer on a

surface of the substrate and further comprises a lipid bearing a first affinity tag at a concentration of greater than or equal to 5 mole percent of the components capable of forming a supported lipid bilayer; and (c) reagents for tethering biological entities to the supported lipid bilayer using a second affinity tag that is capable of binding to the first affinity tag.

[0013] In some aspects, the substrate is fabricated from a material selected from the group consisting of glass, fused-silica, a polymer, or any combination thereof. In some aspects, the first and second affinity tags comprise Ni-NTA and poly-histidine tags. In some aspects, the poly-histidine tag is attached to the N-terminus of a protein. In some aspects, the poly-histidine tag is attached to the C-terminus of a protein. In some aspects, the poly-histidine tag comprises between 4 and 24 histidine residues. In some aspects, the poly-histidine tag comprises 8 histidine residues. In some aspects, the poly-histidine tag comprises 6 histidine residues. In some aspects, the first and second affinity tags comprise biotin- and streptavidin-conjugated reagents. In some aspects, the first and second affinity tags comprise biotin- and avidin-conjugated reagents. In some aspects, the first and second affinity tags comprise biotin- and neutravidin-conjugated reagents. In some aspects, the biological entity is selected from the group consisting of cells, proteins, peptides, receptors, enzymes, antibodies, DNA, RNA, biological molecules, oligonucleotides, small molecules, synthetic molecules, carbohydrates, or any combination thereof. In some aspects, the lipid suspension comprises 1,2-dioleoyl-snglycero-3-phosphocholine. In some aspects, the lipid bearing the first affinity tag comprises 1,2-dioleoyl-sn-glycero-3-[(N-(5-amino-1-carboxypentyl)iminodiacetic acid)succinyl] (nickel salt).

[0014] Also disclosed herein are methods for tethering a biological entity to a substrate comprising: (a) forming a supported lipid bilayer on a surface of a substrate, wherein the supported lipid bilayer comprises an anchor molecule that comprises or bears a first affinity tag; and (b) contacting the supported lipid bilayer with a biological entity present at a concentration less than or equal to 2 uM, or in an amount of less than or equal to 500 ng, wherein the biological entity comprises a nonlinear-active label and a second affinity tag capable of binding to the first affinity tag, thereby tethering the biological entity to the supported lipid bilayer in an oriented fashion. In some aspects, the methods further comprise detecting a non-linear optical signal arising from the tethered biological entity.

[0015] In some aspects, the substrate is fabricated from a material selected from the group consisting of glass, fused-silica, a polymer, or any combination thereof. In some aspects, the first affinity and second affinity tags are Ni-NTA and poly-histidine tags. In some aspects, the

poly-histidine tag is attached to the N-terminus of a protein. In some aspects, the poly-histidine tag is attached to the C-terminus of a protein. In some aspects, the poly-histidine tag comprises between 4 and 24 histidine residues. In some aspects, the poly-histidine tag comprises 8 histidine residues. In some aspects, the poly-histidine tag comprises 6 histidine residues. In some aspects, the first affinity tag comprises Co-CMA and the second affinity tag comprises a poly-histidine tag. In some aspects, the first affinity tag comprises biotin and the second affinity tag comprises streptavidin. In some aspects, the first affinity tag comprises biotin and the second affinity tag comprises avidin. In some aspects, the first affinity tag comprises biotin and the second affinity tag comprises neutravidin. In some aspects, the non-linear optical signal is second harmonic light. In some aspects, the non-linear optical signal is sum frequency light. In some aspects, the non-linear optical signal is difference frequency light. In some aspects, the biological entity is selected from the group consisting of cells, proteins, peptides, receptors, enzymes, antibodies, DNA, RNA, biological molecules, oligonucleotides, small molecules, synthetic molecules, carbohydrates, or any combination thereof. In some aspects, the anchor molecule comprising the first affinity tag is adjusted to a value ranging from 5 mole percent to 100 mole percent of the lipid bilayer. In some aspects, the non-linear optical signal detected increases by at least 5x when the concentration of the anchor molecule comprising the first affinity tag is increased by a factor of 2x. In some aspects, the non-linear optical signal detected increases by at least 10x when the concentration of the anchor molecule comprising the first affinity tag is increased by a factor of 2x. In some aspects, the non-linear optical signal detected increases by at least 20x when the concentration of the anchor molecule comprising the first affinity tag is increased by a factor of 2x. In some aspects, the dependence of the non-linear optical signal on the concentration of the anchor molecule comprising the first affinity tag is described by a power law having an exponent greater than 2. In some aspects, the methods further comprise incubating the supported lipid bilayer with the biological entity for about 10 minutes to about 60 minutes. In some aspects, the biological entity is present at a concentration of about 0.1 uM to 10 uM. In some aspects, the supported lipid bilayer comprises 1,2-dioleoyl-sn-glycero-3-phosphocholine. In some aspects, the anchor molecule conjugated to the first affinity tag comprises 1,2-dioleoyl-sn-glycero-3-[(N-(5-amino-1-carboxypentyl)iminodiacetic acid)succinyl] (nickel salt).

[0016] Disclosed herein are methods for detecting conformational change in a biological entity comprising: (a) illuminating a substrate with one or more light beams at one or more fundamental frequencies, wherein the substrate comprises a supported lipid bilayer, and

wherein the supported lipid bilayer further comprises a Ni-NTA bearing lipid, and wherein a biological entity comprising a non-linear active label and poly-histidine tag is tethered to the supported lipid bilayer by contacting the lipid bilayer with the biological entity at a concentration less than or equal to 2 uM or in an amount less than or equal to 500 ng; (b) measuring a non-linear optical signal arising from the tethered biological entity; (c) optionally contacting the tethered biological entity with one or more candidate binding partners; (d) optionally measuring a non-linear optical signal arising from the tethered biological entity in contact with the one or more candidate binding partners; and (e) optionally comparing the non-linear optical signals measured in steps (b) and (d) to detect a conformational change in the biological entity.

[0017] In some aspects, the substrate is fabricated from a material selected from the group consisting of glass, fused-silica, a polymer, or any combination thereof. In some aspects, the biological entity is a protein and the poly-histidine tag is attached to the N-terminus of the protein. In some aspects, the biological entity is a protein and the poly-histidine tag is attached to the C-terminus of the protein. In some aspects, the poly-histidine tag comprises between 4 and 24 histidine residues. In some aspects, the poly-histidine tag comprises 8 histidine residues. In some aspects, the poly-histidine tag comprises 6 histidine residues. In some aspects, the non-linear optical signal is second harmonic light. In some aspects, the non-linear optical signal is sum frequency light. In some aspects, the non-linear optical signal is difference frequency light. In some aspects, the supported lipid bilayer comprises 1,2-dioleoyl-sn-glycero-3-phosphocholine. In some aspects, the Ni-NTA bearing lipid comprises 1,2-dioleoyl-sn-glycero-3-[(N-(5-amino-1-carboxypentyl)iminodiacetic acid)succinyl] (nickel salt). In some aspects, the biological entity is selected from the group consisting of cells, proteins, peptides, receptors, enzymes, antibodies, DNA, RNA, biological molecules, oligonucleotides, small molecules, synthetic molecules, carbohydrates, or any combination thereof.

INCORPORATION BY REFERENCE

[0018] All publications, patents, and patent applications mentioned in this specification are herein incorporated by reference in their entirety to the same extent as if each individual publication, patent, or patent application was specifically and individually indicated to be incorporated by reference in their entirety. In the event of a conflict between a term herein and a term in an incorporated reference, the term herein controls.

BRIEF DESCRIPTION OF THE DRAWINGS

[0019] The novel features of the disclosed methods and devices are set forth with particularity in the appended claims. A better understanding of the features and advantages of the presently disclosed methods and devices will be obtained by reference to the following detailed description that sets forth illustrative embodiments, in which the principles of the novel designs are utilized, and the accompanying drawings of which:

[0020] FIG. 1A provides a schematic illustration of the energy level diagram for fluorescence (an absorption process).

[0021] FIG. 1B provides a schematic illustration of the energy level diagram for second harmonic generation (a two photon scattering process).

[0022] FIG. 2 provides a schematic illustration of a conformational change in a protein (labeled with a nonlinear-active tag) which is induced by binding of a ligand, and its impact on the distance and/or orientation of a nonlinear-active label relative to an optical interface to which the protein is attached. Incident laser light strikes the surface and through total internal reflection creates an evanescent wave. Labeled protein is bound to the surface and the measured SHG signal magnitude depends on the average, net orientation of the dye label relative to the surface normal (z-axis). A conformational change that re-orients the label results in signal changes.

[0023] FIG. 3 shows a plot of SHG signal intensity for a supported lipid bilayer only, and a supported lipid bilayer having tethered dihydrofolate reductase (DHFR) enzyme labeled with PyMPO-succinimidyl ester (SE) or tethered DHFR enzyme labeled with PyMPO-maleimide (Mal). 5μM enzyme labeled with either PyMPO-maleimide or PyMPO-succinimidyl ester was incubated with a bilayer surface containing 10% Ni-NTA. Each protein was incubated for 60 minutes at room temperature in assay buffer containing 50mM NaPO4 pH 7.0.

[0024] FIG. 4 shows an overlay of 3% and 10% Ni-NTA data to show the relative SHG intensity produced by each protein on the respective surface. The combination of slightly altered incubation conditions and/or increased Ni-NTA percentage provides at least an order of magnitude improvement in the SHG signal for the labeled DHFR enzyme tested here.

[0025] FIG. 5 shows a plot of SHG signal intensity data for PyMPO-labeled, His-tagged maltose binding protein (MBP) tethered to supported lipid bilayers doped with either 3% Ni-NTA-DGS or 10% Ni-NTA-DGS. Dramatic improvement in SHG signal intensity was observed for supported lipid bilayer prepared using a higher Ni-NTA concentration.

[0026] FIG. 6A illustrates characterization of protein immobilization on the bilayer surface. The bar graph shows the intensity of the SHG signal for the model proteins, with and without

imidazole, and for unlabeled protein compared to bilayer. The + denotes the presence of 350 mM imidazole.

[0027] FIG. 6B shows a plot of SHG signal monitored as a function of time after wash-out of excess protein from the bilayer surface.

[0028] FIG. 6C shows a bar graph of the intensity of the SHG signal for incubation of 100 ng of each of the model proteins on the bilayer (N=3).

[0029] FIG. 7A shows a representative SHG time course for addition of calcium binding peptide (CBP) to calmodulin immobilized on an optical interface in the presence of calcium ions. The arrows indicate the time of addition of the indicated compounds.

[0030] FIG. 7B shows a representative SHG time course for addition of calcium binding peptide to immobilized calmodulin in the absence of calcium ions.

[0031] FIG. 7C shows a representative SHG time course for addition of calcium ions followed by addition of calcium binding peptide to immobilized calmodulin.

[0032] FIG. 7D shows a plot of percent changes in SHG signal observed for addition of calcium and CBP; dotted lines represent ± 3σ from the mean of the buffer shifts.

[0033] FIG. 7E shows the crystal structures of free calmodulin (red; pdb 1CFD), Ca-bound calmodulin (orange; pdb 1CLL), and Ca/CBP-bound calmodulin (yellow; pdb 1CDL) shown with the labeled lysine residues identified by mass spectrometry in green. Calcium ions are shown in blue and CBP is shown in purple.

[0034] FIG. 8A shows a representative time course of SHG signal during compound addition to maltose binding protein (MBP) labeled at pH 8.3. The arrows denote the time of injection of buffer, lactose, and maltose.

[0035] FIG. 8B shows a representative time course of SHG signal during compound addition to MBP labeled at pH 7.5. The arrows denote the time of injection of buffer and maltose.

[0036] FIG. 8C shows a plot of the percentage change in SHG signal observed for addition of buffer, lactose, and maltose to MBP. The dotted lines represent ± 3σ standard deviations from the average of the buffer shifts.

[0037] FIG. 8D shows an overlay of the crystal structures of MBP with maltose (blue; pdb 1ANF) and without maltose (orange; pdb 1JW4) bound. Maltose is shown in blue. Modified lysine residues identified by mass spectrometry are shown as sticks in purple on the unbound structure and in green on the bound structure. Many of the labeled lysines are in different conformations in the two crystal structures. For this comparison, the structures were aligned at their N-terminal domains. The His-tag and thus the site of immobilization of the protein is at the N-terminus.

[0038] FIG. 9A shows a representative kinetic trace for methotrexate (MTX) addition to lysine-labeled dihydrofolate reducatase (DHFR). Arrows denote time of addition of buffer and MTX.

[0039] FIG. 9B shows a representative kinetic trace for a TMP-MTX competition experiment for lysine-labeled DHFR. Arrows denote time of addition of buffer, TMP, and MTX.

[0040] FIG. 9C shows a plot of the percent changes in SHG signal observed for buffer, MTX, and TMP addition to lysine-labeled DHFR.

[0041] FIG. 9D shows the crystal structures of the DHFR holoenzyme with (blue; pdb 1RB3) and without (orange; pdb 1RX1) MTX bound. Labeled residues identified by mass spectrometry are shown as sticks in green for DHFR without MTX and in purple for DHFR bound to MTX. MTX is represented in blue.

[0042] FIG. 10A shows a representative time course for MTX addition to cysteine-labeled DHFR.

[0043] FIG. 10B shows a representative kinetic trace for a TMP-MTX competition experiment for cysteine-labeled DHFR. Arrows denote time of addition of buffer, TMP, and MTX.

[0044] FIG. 10C shows a plot of the percentage change in SHG signal observed for buffer, MTX, and TMP addition to cysteine-labeled DHFR.

[0045] FIG. 10D shows the crystal structures of the DHFR holoenzyme with (blue; pdb 1RB3) and without (orange; pdb 1RX1) MTX bound with residue M20 shown in sticks in purple and green for the bound and unbound forms, respectively.

[0046] FIG. 11A shows a standard curve for the fluorescence from cysteine-labeled DHFR.

[0047] FIG. 11B shows a standard curve for the fluorescence from lysine-labeled DHFR.

[0048] FIG. 11C shows a standard curve for the fluorescence from labeled MBP. Tethered and labeled protein attached to the Ni-NTA bilayer was removed from the glass surfaces by serial detergent washes. Cysteine-labeled DHFR, lysine-labeled DHFR, and MBP were all determined to be tethered at surface densities on the order of 1×10^{12} molecules per cm^2.

DETAILED DESCRIPTION

[0049] The methods and compositions disclosed herein provide means for tethering or immobilizing protein molecules on optical interfaces in a manner that ensures both uniform surface coverage of the optical interface and a high degree of orientation of the molecules, thereby providing for significant enhancements of SHG and/or other nonlinear optical signals arising from the tethered protein molecules, as well as improved signal-to-noise ratios.

[0050] In some aspects of the present disclosure, methods are described for determining orientation, conformation, or changes in orientation or conformation of biological entities in response to contacting the biological entities with one or more test entities. As used herein, determining orientation, conformation, or changes thereof may involve measurement of a nonlinear optical signal which is related to and/or proportional to the average orientation of a nonlinear-active label or tag. In general, the methods disclosed rely on the use of second harmonic generation (SHG) or related nonlinear optical techniques (e.g. sum frequency generation (SFG) or difference frequency generation (DFG)) for detection of orientation, conformation, or conformational change, as described previously, for example, in U.S. Patent Nos. 6,953,694, and 8,497,703.

Detection of Conformation Using Second Harmonic Generation

[0051] Second harmonic generation, in contrast to more widely used fluorescence-based techniques (FIG. 1A), is a nonlinear optical process, in which two photons of the same excitation wavelength or frequency interact with a nonlinear material and are re-emitted as a single photon having twice the energy, *i.e.* twice the frequency and half the wavelength, of the excitation photons (FIG. 1B). Second harmonic generation only occurs in nonlinear materials lacking inversion symmetry (*i.e.* in non-centrosymmetric materials), and requires a high intensity excitation light source. It is a special case of sum frequency generation, and is related to other nonlinear optical phenomena such as difference frequency generation.

[0052] Second harmonic generation and other nonlinear optical techniques can be configured as surface-selective detection techniques because of their dependence on the orientation of the nonlinear-active species. Tethering of the nonlinear-active species to a planar surface, for example, can instill an overall degree of orientation that is absent when molecules are free to undergo rotational diffusion in solution. An equation commonly used to model the orientation-dependence of nonlinear-active species at an interface is:

$$\chi^{(2)} = N_s\langle\alpha^{(2)}\rangle \quad (1)$$

where $\chi^{(2)}$ is the nonlinear susceptibility, N_s is the total number of nonlinear-active molecules per unit area at the interface, and $\langle\alpha^{(2)}\rangle$ is the average orientation of the nonlinear hyperpolarizability ($\alpha^{(2)}$) of these molecules. The intensity of SHG is proportional to the square of the nonlinear susceptibility, and is thus dependent on both the number of oriented nonlinear-active species at the interface and on changes in their average orientation.

[0053] Second harmonic generation and other nonlinear optical techniques may be rendered additionally surface selective through the use of total internal reflection as the mode for delivery of the excitation light to the optical interface on which nonlinear-active species have been immobilized. Total internal reflection of the incident excitation light creates an "evanescent wave" at the interface, which may be used to selectively excite only nonlinear-active labels that are in close proximity to the surface, *i.e.* within the spatial decay distance of the evanescent wave, which is typically on the order of tens of nanometers. Total internal reflection may also be used to excite fluorescence in a surface-selective manner, for example to excite a fluorescence donor attached to the optical interface, which then transfers energy to a suitable acceptor molecule via a fluorescence resonance energy transfer (FRET) mechanism. In the present disclosure, the evanescent wave generated by means of total internal reflection of the excitation light is preferentially used to excite a nonlinear-active label or molecule. The efficiency of exciting nonlinear active species depends strongly on both their average orientation and on their proximity to the interface.

[0054] This surface selective property of SHG and other nonlinear optical techniques can be exploited to detect conformational changes in biological molecules immobilized at interfaces. For example, a conformational change in a receptor molecule that results from binding of a ligand to the receptor might be detected using a nonlinear-active label or moiety, where the label is attached to or associated with the receptor in such a way that the conformational change leads to a change in the orientation or distance of the label with respect to the interface (FIG. 2), and thus to a change in a physical property of the nonlinear optical signal. In the past, the use of surface-selective nonlinear optical techniques has been confined mainly to applications in physics and chemistry, since relatively few biological samples are intrinsically non-linearly active. Recently, the use of second harmonic active labels ("SHG labels") has been introduced, allowing virtually any molecule or particle to be rendered highly non-linear active. The first example of this was demonstrated by labeling the protein cytochrome c with an oxazole dye and detecting the protein conjugate at an air-water interface with second harmonic generation (Salafsky (2006), Chem. Physics Letters 342(5-6):485-491) . Surface-selective nonlinear optical techniques are also coherent techniques, meaning that the fundamental and nonlinear optical light beams have wave fronts that propagate through space with well-defined spatial and phase relationships. The use of surface-selective nonlinear optical detection techniques for analysis of conformation of biological molecules or other biological entities has a number of inherent advantages over other optical approaches, including: i) sensitive and direct dependence of the nonlinear signal

on the orientation and/or dipole moment(s) of the nonlinear-active species, thereby conferring sensitivity to conformational change; (ii) higher signal-to-noise (lower background) than fluorescence-based detection since the nonlinear optical signal is generated only at surfaces that create a non-centrosymmetric system, i.e. the technique inherently has a very narrow "depth-of-field"; (iii) as a result of the narrow "depth of field", the technique is useful when measurements must be performed in the presence of a overlaying solution, e.g. where a binding process might be obviated or disturbed by a separation or rinse step. This aspect of the technique may be particularly useful for performing equilibrium binding measurements, which require the presence of bulk species, or kinetics measurements where the measurements are made over a defined period of time; (iv) the technique exhibits lower photo-bleaching and heating effects than those that occur in fluorescence, due to the facts that the two-photon absorption cross-section is typically much lower than the one-photon absorption cross-section for a given molecule, and that SHG (and sum frequency generation or difference frequency generation) involves scattering, not absorption; (v) minimal collection optics are required and higher signal to noise is expected since the fundamental and nonlinear optical beams (e.g., second harmonic light) have well-defined incoming and outgoing directions with respect to the interface. This is particularly advantageous compared to fluorescence-based detection, as fluorescence emission is isotropic and there may also be a large fluorescence background component to detected signals arising from out-of-focal plane fluorescent species.

Biological Entities and Test Entities

[0055] The methods and compositions disclosed herein are often applied to the tethering or immobilization of proteins. However, in some embodiments they may also be applied to tethering or immobilization of other biological entities. As used herein, the phrase "biological entities" comprises but is not limited to cells, proteins, peptides, receptors, enzymes, antibodies, DNA, RNA, biological molecules, oligonucleotides, small molecules, synthetic molecules, carbohydrates, or any combination thereof. Similarly, the phrase "test entities" also comprises but is not limited to cells, proteins, peptides, receptors, enzymes, antibodies, DNA, RNA, biological molecules, oligonucleotides, solvents, small molecules, synthetic molecules, carbohydrates, or any combination thereof. In some aspects, biological entities may comprise drug targets, or portions thereof, while test entities may comprise drug candidates, or portions thereof.

Nonlinear-Active Labels and Labeling Techniques

[0056] As noted above, most biological molecules are not intrinsically nonlinear-active. Exceptions include collagen, a structural protein that is found in most structural or load-bearing tissues. SHG microscopy has been used extensively in studies of collagen-containing structures, for example, the cornea. Other biological molecules or entities must be rendered nonlinear-active by means of introducing a nonlinear-active moiety such as a tag or label. A label for use in the presently disclosed methods refers to a nonlinear-active moiety, tag, molecule, or particle which can be bound, either covalently or non-covalently, to a molecule, particle, or phase (e.g., a lipid bilayer) in order to render the resulting system more nonlinear optical active. Labels can be employed in the case where the molecule, particle or phase (e.g., lipid bilayer) is not nonlinear active to render the system nonlinear-active, or with a system that is already nonlinear-active to add an extra characterization parameter to the system. Exogenous labels can be pre-attached to the molecules, particles, or other biological entities, and any unbound or unreacted labels separated from the labeled entities before use in the methods described herein. In a specific aspect of the methods disclosed herein, the nonlinear-active moiety is attached to the target molecule or biological entity in vitro prior to immobilizing the target molecules or biological entities in discrete regions of the substrate surface. The labeling of biological molecules or other biological entities with nonlinear-active labels allows a direct optical means of detecting interactions between the labeled biological molecule or entity and another molecule or entity (i.e. the test entity) in cases where the interaction results in a change in orientation or conformation of the biological molecule or entity using a surface-selective nonlinear optical technique.

[0057] In alternative aspects of the methods and systems described herein, at least two distinguishable nonlinear-active labels are used. The orientation of the attached two or more distinguishable labels would then be chosen to facilitate well defined directions of the emanating coherent nonlinear light beam. The two or more distinguishable labels can be used in assays where multiple fundamental light beams at one or more frequencies, incident with one or more polarization directions relative to the optical interface are used, with the resulting emanation of at least two nonlinear light beams.

[0058] Examples of nonlinear-active tags or labels include, but are not limited to, the compounds listed in Table 1, and their derivatives.

Table 1. Examples of Nonlinear-Active Tags

2-aryl-5-(4-pyridyl)oxazole	Hemicyanines	Polyimides
2-(4-pyridyl)-cycloalkano[d]oxazoles	lndandione-1 ,3-pyidinium betaine	Polymethacrylates
5-aryl-2-(4-pyridyl)oxazole	lndodicarbocyanines	PyMPO (pyridyloxazole)
7-Hydroxycoumarin-3-carboxylic acid, succinimidyl ester	Melamines	PyMPO, succinimidyl ester (1-(3-(succinimidyloxycarbonyl)benzyl)-4-(5-(4-PyMPO, maleimide
Azo dyes	Merocyanines	Stilbazims
Benzooxazoles	Methoxyphenyl)oxazol-2-yl)pyridinium bromide)	Stilbenes
Bithiophenes	Methylene blue	Stryryl-based dyes
Cyanines	Oxazole or oxadizole molecules	Sulphonyl-substituted azobenzenes
Dapoxyl carboxylic acid, succinimidyl ester	Oxonols	Thiophenes
Diaminobenzene compounds	Perylenes	Tricyanovinyl aniline
Diazostilbenes	Phenothiazine-stilbazole	Tricyanovinyl azo
Fluoresceins	Polyenes	

[0059] In evaluating whether a species may be nonlinear-active, the following characteristics can indicate the potential for nonlinear activity: a large difference dipole moment (difference in dipole moment between the ground and excited states of the molecule), a large Stokes shift in fluorescence, or an aromatic or conjugated bonding character. In further evaluating such a species, an experimenter can use a simple technique known to those skilled in the art to confirm the nonlinear activity, for example, through detection of SHG from an air-water interface on which the nonlinear-active species has been distributed. Once a suitable nonlinear-active species bas been selected for the experiment at hand, the species can be conjugated, if desired, to a biological molecule or entity for use in the surface-selective nonlinear optical methods and systems disclosed herein.

[0060] The following reference and references therein describe techniques available for creating a labeled biological entity from a synthetic dye and many other molecules: Greg T. Hermanson, Bioconjugate Techniques, Academic Press. 1996.

[0061] In a specific aspect of the methods and systems disclosed, metal nanoparticles and assemblies thereof are modified to create biological nonlinear-active labels. The following references describe the modification of metal nanoparticles and assemblies: J.P. Novak and

D. L. Feldheim, "Assembly of Phenylacetylene-Bridged Silver and Gold Nanoparticle Arrays". J. Am. Chem. Soc., 2000, 122, 3979-3980; J.P. Novak et al., "Nonlinear Optical Properties of Molecularly Bridged Gold Nanoparticle Arrays". J. Am. Chem. Soc. 2000, 122, 12029-12030; Vance, F W, Lemon B. I., Hupp, J. T., " Enormous Hyper-Rayleigh Scattering from Nanocrystalline Gold Particle Suspensions". J. Phys. Chem. B 102:10091-93 (1999).

[0062] In yet another aspect of the methods and systems disclosed herein, the nonlinear activity of the system can also be manipulated through the introduction of nonlinear analogues to molecular beacons, that is, molecular beacon probes that have been modified to incorporate a nonlinear-active label (or modulator thereof) instead of fluorophores and quenchers. These nonlinear optical analogues of molecular beacons are referred to herein as molecular beacon analogues (MB analogues or MBA). The MB analogues to be used in the described methods and systems can be synthesized according to procedures known to one of ordinary skill in the art.

Types of Biological Interactions Detected

[0063] The methods and systems disclosed herein provide for detection of a variety of interactions between biological entities, or between biological entities and test entities, depending on the choice of biological entities, test entities, and non-linear active labeling technique employed. In one aspect, the present disclosure provides for the qualitative detection of binding events, e.g. the binding of a ligand to a receptor, as indicated by the resulting conformational change induced in the receptor. In another aspect, the present disclosure provides for quantitative analysis of binding events, e.g. the binding of a ligand to a receptor, by performing replicate measurements using different concentrations of the ligand molecule and generating a dose-response curve using the percent change in maximal conformational change observed. Similarly, other aspects of the present disclosure may provide methods for qualitative or quantitative measurements of enzyme-inhibitor interactions, antibody-antigen interactions, the formation of complexes of biological macromolecules, or interactions of receptors with allosteric modulators.

[0064] In other specific embodiments, MB analogues can be used according to the methods disclosed herein as hybridization probes that can detect the presence of complementary nucleic acid target without having to separate probe-target hybrids from excess probes as in solution-phase hybridization assays, and without the need to label the targets oligonucleotides. MB analogue probes can also be used for the detection of RNAs within living cells, for monitoring the synthesis of specific nucleic acids in sample aliquots drawn

from bioreactors, and for the construction of self-reporting oligonucleotide arrays. They can be used to perform homogeneous one-well assays for the identification of single-nucleotide variations in DNA and for the detection of pathogens or cells immobilized to surfaces for interfacial detection.

[0065] Interactions between biological entities or biological and test entities (e.g. binding reactions, conformational changes, etc.) can be correlated through the methods presently disclosed to the following measurable nonlinear signal parameters: (i) the intensity of the nonlinear light, (ii) the wavelength or spectrum of the nonlinear light, (iii) the polarization of the nonlinear light, (iv) the time-course of (i), (ii), or (iii), and/or vi) one or more combinations of (i), (ii), (iii), and (iv).

Substrate Formats, Optical Interface, and Total Internal Reflection

[0066] As described above, the systems and methods of the present disclosure typically utilize a planar substrate for immobilization of one or more biological entities on a top surface of the substrate, wherein the top substrate surface further comprises the optical interface (or sample interface) used for exciting nonlinear optical signals. The substrate can be glass, silica, fused-silica, plastic, or any other solid material that is transparent to the fundamental and second harmonic light beams, and that supports total internal reflection at the substrate/sample interface when the excitation light is incident at an appropriate angle.

[0067] In some aspects of the disclosed immobilization chemistries, the substrate (or solid support) upon which biological entities are immobilized may be non-planar, for example, the substrate may comprise a convex, concave, or irregular surface, or may comprise glass beads, polymer beads, and the like. A bead or particle may comprise any type of solid, porous, or hollow bead or particle. A bead or particle may comprise a discrete shape that may be spherical (*e.g.*, a microsphere) or have a non-spherical or irregular shape, such as cubic, cuboid, pyramidal, cylindrical, conical, oblong, or disc-shape, and the like. A bead or particle may refer to any three dimensional structure that provides an increased surface area for immobilization of biological entities. Beads or particles may comprise a variety of materials including, but not limited to, paramagnetic materials (*e.g.* magnesium, molybdenum, lithium, and tantalum), superparamagnetic materials (*e.g.* ferrite (Fe_3O_4); magnetite nanoparticles), ferromagnetic materials (*e.g.* iron, nickel, cobalt, some alloys thereof, and some rare earth metal compounds), ceramic, plastic, glass, polystyrene, silica, methylstyrene, acrylic polymers, titanium, latex, sepharose, agarose, hydrogel, polymer, cellulose, nylon, and any combination thereof.

[0068] In some aspects of the disclosed methods, the biological entities may be immobilized uniformly across a substrate surface. In other embodiments, the biological entities may be immobilized in one or more discrete regions of a substrate surface. In some embodiments, the discrete regions within which biological entities are contained are configured as one-dimensional or two-dimensional arrays, or are distributed randomly across the substrate surface, and are separated from one another by means of a hydrophobic coating or thin metal layer. In other aspects, the discrete regions may comprise indents in the substrate surface. In still other aspects, the discrete regions may be separated from each other by means of a well-forming component such that the substrate forms the bottom of a microwell plate (or microplate), and each individual discrete region forms the bottom of one well in the microwell plate. In one aspect of the present disclosure, the well-forming component separates the top surface of the substrate into 96 separate wells. In another aspect, the well-forming component separates the top surface of the substrate into 384 wells. In yet another aspect, the well-forming component separates the top surface of the substrate into 1,536 wells. In all of these aspects, the substrate, whether configured in a planar array, indented array, or microwell plate format, may comprise a disposable or consumable device or cartridge that interfaces with other optical and mechanical components of a high throughput analysis system.

[0069] The methods and systems disclosed herein further comprise specifying the number of discrete regions or wells into which the substrate surface is divided, irrespective of how separation is maintained between discrete regions or wells. Having larger numbers of discrete regions or wells on a substrate may be advantageous in terms of increasing the sample analysis throughput of the method or system. In one aspect of the present disclosure, the number of discrete regions or wells per substrate is between 10 and 1,600. In other aspects, the number of discrete regions or wells is at least 10, at least 20, at least 50, at least 100, at least 200, at least 300, at least 400, at least 500, at least 750, at least 1,000, at least 1,250, at least 1,500, or at least 1,600. In yet other aspects of the disclosed methods and systems, the number of discrete regions or wells is at most 1,600, at most 1,500, at most 1,000, at most 750, at most 500, at most 400, at most 300, at most 200, at most 100, at most 50, at most 20, or at most 10. In a preferred aspect, the number of discrete regions or wells is 96. In another preferred aspect, the number of discrete regions or wells is 384. In yet another preferred aspect, the number of discrete regions or wells is 1,536. Those of skill in the art will appreciate that the number of discrete regions or wells may fall within any range bounded by any of these values (e.g. from about 12 to about 1,400).

[0070] The methods and systems disclosed herein also comprise specifying the surface area of the discrete regions or wells into which the substrate surface is divided, irrespective of how separation is maintained between discrete regions or wells. Having discrete regions or wells of larger area may facilitate ease-of-access and manipulation of the associated biological entities in some cases, whereas having discrete regions or wells of smaller area may be advantageous in terms of reducing assay reagent volume requirements and increasing the sample analysis throughput of the method or system. In one aspect of the present disclosure, the surface area of the discrete regions or wells is between 1 mm^2 and 100 mm^2. In other aspects, the area of the discrete regions or wells is at least 1 mm^2, at least 2.5 mm^2, at least 5 mm^2, at least 10 mm^2, at least 20 mm^2, at least 30 mm^2, at least 40 mm^2, at least 50 mm^2, at least 75 mm^2, or at least 100 mm^2. In yet other aspects of the disclosed methods and systems, the area of the discrete regions or wells is at most 100 mm^2, at most 75 mm^2, at most 50 mm^2, at most 40 mm^2, at most 30 mm^2, at most 20 mm^2, at most 10 mm^2, at most 5 mm^2, at most 2.5 mm^2, or at most 1 mm^2. In a preferred aspect, the area of discrete regions or wells is about 35 mm^2. In another preferred aspect, the area of the discrete regions or wells is about 8.6 mm^2. Those of skill in the art will appreciate that the area of the discrete regions or wells may fall within any range bounded by any of these values (e.g. from about 2 mm^2 to about 95 mm^2).

[0071] In some embodiments, one or more discrete regions of the substrate surface are simultaneously exposed to (illuminated with) excitation light. In other embodiments, one or more discrete regions of the substrate surface are sequentially exposed to (illuminated with) excitation light by re-positioning the substrate relative to the excitation light source. Total internal reflection of the incident excitation light creates an "evanescent wave" at the sample interface, which excites the nonlinear-active labels immobilized thereon, and results in generation of second harmonic light (or in some aspects sum frequency or difference frequency light). Because the intensity of the evanescent wave, and hence the intensity of the nonlinear optical signals generated, is dependent on the incident angle of the excitation light beam, precise orientation of the substrate plane with respect to the optical axis of the excitation beam and efficient optical coupling of the beam to the substrate is critical for achieving optimal SHG signal across the array of discrete regions. In some aspects of the present disclosure, total internal reflection is achieved by means of a single reflection of the excitation light from the substrate surface. In other aspects, the substrate may be configured as a waveguide such that the excitation light undergoes multiple total internal reflections as it propagates along the waveguide. In yet other aspects, the substrate may be configured as a

zero-mode waveguide, wherein an evanescent field is created by means of nanofabricated structures.

[0072] Efficient optical coupling between the excitation light beam and the substrate is often achieved by use of an index-matching fluid such as mineral oil, mixtures of mineral oil and hydrogenated terphenyls, perfluorocarbon fluids, glycerin, glycerol, or similar fluids having a refractive index near 1.5, wherein the index-matching fluid is wicked between a prism used to guide the light beam and the lower surface of the substrate. Alternative approaches for creating efficient optical coupling of the excitation beam to the substrate in high throughput systems are described in U.S Patent Application No. 14/754,465.

Immobilization Chemistries

[0073] As disclosed herein, substrates in any of the formats described above are further configured for immobilization of biological entities across at least one surface of the substrate or within specified discrete regions of a substrate surface. Immobilization of biological molecules or cells may be accomplished by a variety of techniques known to those of skill in the art, for example, through the use of aminopropyl silane chemistries to functionalize glass or fused-silica surfaces with amine functional groups, followed by covalent coupling using amine-reactive conjugation chemistries, either directly with the biological molecule of interest, or via an intermediate spacer or linker molecule. Non-specific adsorption may also be used directly or indirectly, e.g. through the use of BSA-N-hydroxysuccinimide (BSA-NHS) by first attaching a molecular layer of BSA to the surface and then activating it with N,N'-disuccinimidyl carbonate. The activated lysine, aspartate or glutamate residues on the BSA react with surface amines on proteins.

[0074] In a preferred aspect of the present disclosure, biological molecules may be immobilized on the surface by means of tethering to or embedding in "supported lipid bilayers", the latter comprising small patches of lipid bilayer confined to a silicon or glass surface by means of hydrophobic and electrostatic interactions, where the bilayer is "floating" above the substrate surface on a thin layer of aqueous buffer. Supported phospholipid bilayers can also be prepared with or without membrane proteins or other membrane-associated components as described, for example, in Salafsky *et al.* "Architecture and Function of Membrane Proteins in Planar Supported Bilayers: A Study with Photosynthetic Reaction Centers", Biochemistry 35 (47): 14773-14781 (1996); Gennis, R., Biomembranes, Springer-Verlag, 1989; Kalb *et al.*, "Formation of Supported Planar Lipid Bilayers by Fusion of Vesicles to Supported Phospholipid Monolayers", Biochimica

Biophysica Acta 1103:307-316 (1992); and Brian *et al.*, "Allogeneic Stimulation of Cyto-toxic T-cells by Supported Planar Membranes." PNAS-Biological Sciences 81(19): 6159-6163 (1984). Supported phospholipid bilayers are well known in the art and there are numerous techniques available for their fabrication. Potential advantages of using supported lipid bilayers for immobilization of proteins or other biological entities on substrate surfaces or optical interfaces include (i) preservation of membrane protein structure for those proteins that typically span the cell membrane or other membrane components of cells and require interaction with the hydrophobic core of the bilayer for stabilization of secondary and tertiary structure, (ii) preservation of two dimensional lateral and rotational diffusional mobility for studying interactions between protein components within the bilayer, and (iii) preservation of molecular orientation, depending on such factors as the type of protein under study (i.e. membrane or soluble protein), how the bilayer membrane is formed on the substrate surface, and how the protein is tethered to the bilayer (in the case of soluble proteins). Supported bilayers, with or without tethered or embedded protein, should typically be submerged in aqueous solution to prevent their destruction when exposed to air.

[0075] Soluble proteins and other biological entities may be tethered or attached to the supported lipid bilayer in an oriented fashion using a number of different anchor molecules, linkers, and/or attachment chemistries. As used herein, “anchor molecules” are molecules which are embedded in the lipid bilayer, and may comprise fatty acid, glycerolipid, glycerophospholipid, sphingolipid, or other lipid or non-lipid molecules to which attachment moieties are conjugated. The concentration of anchor molecules in the supported lipid bilayer may range from about 1 mole percent to as much as 100 mole percent. In some embodiments, the concentration of anchor molecules in the supported lipid bilayer may be at least 1 mole percent, at least 2.5 mole percent, at least 5 mole percent, at least 10 mole percent, at least 20 mole percent, at least 30 mole percent, at least 40 mole percent, at least 50 mole percent, at least 60 mole percent, at least 70 mole percent, at least 80 mole percent, at least 90 mole percent, or 100 mole percent. In some embodiments, the concentration of anchor molecules in the supported lipid bilayer may be at most 100 mole percent, at most 90 mole percent, at most 80 mole percent, at most 70 mole percent, at most 60 mole percent, at most 50 mole percent, at most 40 mole percent, at most 30 mole percent, at most 20 mole percent, at most 10 mole percent, at most 5 mole percent, at most 2.5 mole percent, or at most 1 mole percent. Those of skill in the art will recognize that the concentration of anchor molecules in the supported lipid bilayer may have any value within this range, for example, about 8.5 mole percent.

[0076] Linker molecules are molecules used to provide spatial ("vertical") separation between the attachment point of the protein or other biological entity being tethered and the attachment point on the anchor molecule embedded in the plane of the lipid bilayer. Examples of suitable linker molecules include, but are not limited to, omega-amino fatty acids, polyethylene glycols, and the like.

[0077] Attachment moieties (also referred to as "affinity tags") are specific chemical structures or binding partners that provide for covalent or non-covalent binding between two biological entities. Examples of attachment moieties or affinity tags that are suitable for use in the methods disclosed herein include biotin and avidin (or biotin and streptavidin), and His-tag / Ni-NTA binding partners.

[0078] The high affinity, non-covalent biotin-streptavidin interaction is widely used in biological assay techniques to conjugate or immobilize proteins or other biological entities. Biotinylation of proteins enables capture by multivalent avidin or streptavidin molecules that are themselves adhered to a surface (e.g. glass slides or beads) or conjugated to another molecule (e.g. through the use of a biotin-streptavidin-biotin bridge or linker). The biotin moiety is sufficiently small that biotinylation typically doesn't interfere with protein function. The high affinity (K_d of 10^{-14} M to 10^{-15}M) and high specificity of the binding interaction between biotin and avidin or streptavidin enables capture of biotinylated proteins of interest even from complex samples. Due to the extremely strong binding interaction, harsh conditions are needed to elute biotinylated protein from streptavidin-coated surfaces (typically 6M guanidine HCl at pH 1.5), which will often denature the protein of interest. The use of monomeric forms of avidin or streptavidin, which have a decreased biotin-binding affinity of ~10^{-8} M, may allow biotinylated proteins to be eluted with excess free biotin if necessary. In the methods disclosed herein, lipid molecules comprising biotin moieties may be incorporated into supported lipid bilayers for the purpose of immobilizing or tethering biotinylated proteins and/or other biotinylated biological entities to the bilayer via a biotin-avidin-biotin (or biotin-streptavidin-biotin) bridge.

[0079] Biotinylation of proteins and other biological entities may be performed by direct coupling, e.g. through conjugation of primary amines on the surface of a protein using N-hydroxysuccinimidobiotin (NHS-biotin). Alternatively, recombinant proteins are conveniently biotinylated using the AviTag approach, wherein the AviTag peptide sequence (GLNDIFEAQKIEWHE) is incorporated into the protein through the use of genetic engineering and protein expression techniques. The presence of the AviTag sequence allows biotinylation of the protein by treatment with the BirA enzyme.

[0080] His tag chemistry is another widely used tool for purification of recombinant proteins and other biomolecules. In this approach, a DNA sequence specifying a string of six to nine histidine residues, for example, may be incorporated into vectors used for production of recombinant proteins comprising 6xHis or poly-His tags fused to their N- or C-termini. His-tagged proteins can then be purified and detected as a result of the fact that the string of histidine residues binds to several types of immobilized metal ions, including nickel, cobalt and copper, under specific buffer conditions. Supports such as agarose beads or magnetic particles can be derivatized with chelating groups to immobilize the desired metal ions, which then function as ligands for binding and purification of the His-tagged biomolecules of interest. In the methods disclosed herein, the number of histidine residues incorporated into recombinant proteins may range from 1 residue to 24 residues, or more. In some embodiments, the number of histidine residues incorporated may be at least 1 residue, at least 2 residues, at least 4 residues, at least 6 residues, at least 8 residues, at least 10 residues, at least 12 residues, at least 14 residues, at least 16 residues, at least 18 residues, at least 20 residues, at least 22 residues, or at least 24 residues. In some embodiments, the number of histidine residues incorporated may be at most 24 residues, at most 22 residues, at most 20 residues, at most 18 residues, at most 16 residues, at most 14 residues, at most 12 residues, at most 10 residues, at most 8 residues, at most 6 residues, at most 4 residues, at most 2 residues, or at most 1 residue. Those of skill in the art will recognize that the number of histidine residues incorporated may have any value within this range, for example, 7 residues.

[0081] The chelators most commonly used to create His-tag ligands are nitrilotriacetic acid (NTA) and iminodiacetic acid (IDA). Once NTA- or IDA-conjugated supports are prepared, they can be "loaded" with the desired divalent metal (e.g., Ni, Co, Cu, or Fe). When using nickel as the metal, for example, the resulting affinity support is usually called a Ni-chelate, Ni-IDA or Ni-NTA support. Affinity purification of His-tagged fusion proteins is the most common application for metal-chelate supports in protein biology research. Nickel or cobalt metals immobilized by NTA-chelation chemistry are the systems of choice for this application.

[0082] In the methods disclosed herein, lipid molecules comprising Ni-NTA groups (or other chelated metal ions) may be incorporated into supported lipid bilayers for the purpose of immobilizing or tethering His-tagged proteins and other His-tagged biological entities to the bilayer. In some embodiment, the supported lipid bilayer may comprise, for example, 1,2-dioleoyl-sn-glycero-3-phosphocholine, and may also contain, for example, 1,2-dioleoyl-sn-glycero-3-[(N-(5-amino-1-carboxypentyl)iminodiacetic acid)succinyl] (nickel salt) at various

concentrations. The concentration of 1,2-dioleoyl-sn-glycero-3-[(N-(5-amino-1-carboxypentyl)iminodiacetic acid)succinyl] (nickel salt) in the supported lipid bilayer may range from as little as 1 mole percent to as much as 100 mole percent. In some embodiments, the concentration of 1,2-dioleoyl-sn-glycero-3-[(N-(5-amino-1-carboxypentyl)iminodiacetic acid)succinyl] (nickel salt) may be at least 1 mole percent, at least 2.5 mole percent, at least 5 mole percent, at least 10 mole percent, at least 20 mole percent, at least 30 mole percent, at least 40 mole percent, at least 50 mole percent, at least 60 mole percent, at least 70 mole percent, at least 80 mole percent, at least 90 mole percent, or 100 mole percent. In some embodiments, the concentration of 1,2-dioleoyl-sn-glycero-3-[(N-(5-amino-1-carboxypentyl)iminodiacetic acid)succinyl] (nickel salt) in the supported lipid bilayer may be at most 100 mole percent, at most 90 mole percent, at most 80 mole percent, at most 70 mole percent, at most 60 mole percent, at most 50 mole percent, at most 40 mole percent, at most 30 mole percent, at most 20 mole percent, at most 10 mole percent, at most 5 mole percent, at most 2.5 mole percent, or at most 1 mole percent. Those of skill in the art will recognize that the concentration of 1,2-dioleoyl-sn-glycero-3-[(N-(5-amino-1-carboxypentyl)iminodiacetic acid)succinyl] (nickel salt) in the supported lipid bilayer may have any value within this range, for example, about 5.5 mole percent.

[0083] Poly-His tags bind best to chelated metal ions in near-neutral buffer conditions (physiologic pH and ionic strength). A typical binding/wash buffer consists of Tris-buffer saline (TBS) pH 7.2, containing 10-25mM imidazole. The low-concentration of imidazole helps to prevent nonspecific binding of endogenous proteins that have histidine clusters. Elution and recovery of captured His-tagged protein from chelated metal ion supports, when desired, is typically accomplished using a high concentration of imidazole (at least 200mM), low pH (e.g., 0.1M glycine-HCl, pH 2.5), or an excess of strong chelator (e.g., EDTA). Immunoglobulins are known to have multiple histidines in their Fc region and can bind to chelated metal ion supports, therefore stringent binding conditions (e.g. using an appropriate concentration of imidazole) are necessary to avoid high levels of background binding if immunoglobulins are present in a sample at high relative abundance compared to the His-tagged proteins of interest. Albumins, such as bovine serum albumin (BSA), also have multiple histidines and can yield high levels of background binding to chelated metal ion supports in the absence of more abundant His-tagged proteins or the use of imidazole in the binding/wash buffer.

Control of Surface Density of Immobilized Biological Entities

[0084] In some embodiments of the disclosed methods, it may sometimes be desirable to vary the surface density of proteins or other biological entities that are immobilized on or tethered to the substrate surface comprising the optical interface. This can be accomplished in a variety of ways, as is well known to those of skill in the art. For example, in embodiments where proteins (or other biological entities) are coupled to the surface through the use of aminopropyl silane chemistries to functionalize glass or fused-silica surfaces with amine functional groups, followed by covalent coupling using amine-reactive conjugation chemistries and linker molecules, the ratio of bi-functional (*e.g.* comprising both a primary amine and carboxyl functional group) to mono-functional (*e.g.* comprising only a carboxyl functional group) linkers in the reaction mixture may be varied to control the surface density of primary amine functional groups available for coupling with the protein.

[0085] As another example, in embodiments of the disclosed methods where biotin-streptavidin binding interactions are used to tether biotinylated proteins to biotinylated lipid molecules incorporated into a supported lipid bilayer (via a biotin-streptavidin-biotin bridge), the mole percent of the biotinylated lipid molecule used to form the bilayer may be varied in order to control the surface density of biotin groups available for binding. The concentration of biotinylated lipid molecules may range from as little as 1 mole percent to as much as 100 mole percent. In some embodiments, the concentration of biotinylated lipid molecule in the supported lipid bilayer may be at least 1 mole percent, at least 2.5 mole percent, at least 5 mole percent, at least 10 mole percent, at least 20 mole percent, at least 30 mole percent, at least 40 mole percent, at least 50 mole percent, at least 60 mole percent, at least 70 mole percent, at least 80 mole percent, at least 90 mole percent, or 100 mole percent. In some embodiments, the concentration of biotinylated lipid molecule in the supported lipid bilayer may be at most 100 mole percent, at most 90 mole percent, at most 80 mole percent, at most 70 mole percent, at most 60 mole percent, at most 50 mole percent, at most 40 mole percent, at most 30 mole percent, at most 20 mole percent, at most 10 mole percent, at most 5 mole percent, at most 2.5 mole percent, or at most 1 mole percent. Those of skill in the art will recognize that the concentration of biotinylated lipid molecule in the supported lipid bilayer may have any value within this range, for example, about 8 mole percent. Alternatively, the concentration and/or incubation time used for attaching streptavidin to the biotinylated lipid bilayer (or for attaching the biotinylated protein to the tethered streptavidin molecules) may be varied. The concentration of streptavidin or biotinylated protein used may range from about 0.1 μM to about 10 μM, or more. In some embodiments, the concentration of

streptavidin or biotinylated protein used may be at least 0.1 μM, at least 0.5 μM, at least 1 μM, at least 2 μM, at least 3 μM, at least 4 μM, at least 5 μM, at least 6 μM, at least 7 μM, at least 8 μM, at least 9 μM, or at least 10 μm. In some embodiments, the concentration of streptavidin or biotinylated protein used may be at most 10 μM, at most 9 μM, at most 8 μM, at most 7 μM, at most 6 μM, at most 5 μM, at most 4 μM, at most 3 μM, at most 2 μM, at most 1 μM, at most 0.5 μM, or at most 0.1 μM. Those of skill in the art will recognize that the concentration of streptavidin or biotinylated protein used may have any value within this range, for example, about 4.4 μM. Expressed in terms of the amount of streptavidin or biotinylated protein used for attachment, the amount may range from about 1 nanogram to about 1,000 nanograms, or more. In some embodiment, the amount of streptavidin or biotinylated protein used for attachment may be at least 1 nanogram, at least 10 nanograms, at least 25 nanograms, at least 75 nanograms, at least 100 nanograms, at least 200 nanograms, at least 300 nanograms, at least 400 nanograms, at least 500 nanograms, at least 600 nanograms, at least 700 nanograms, at least 800 nanograms, at least 900 nanograms, or at least 1,000 nanograms. In some embodiments, the amount of streptavidin or biotinylated protein used for attachment may be at most 1,000 nanograms, at most 900 nanograms, at most 800 nanograms, at most 700 nanograms, at most 600 nanograms, at most 500 nanograms, at most 400 nanograms, at most 300 nanograms, at most 200 nanograms, at most 100 nanograms, at most 75 nanograms, at most 50 nanograms, at most 25 nanograms, at most 10 nanograms, or at most 1 nanogram. Those of skill in the art will recognize that the amount of streptavidin or biotinylated protein used for attachment may have any value within this range, for example, about 275 nanograms. The incubation time used for attaching streptavidin or biotinylated protein may range from about 10 minutes to about 60 minutes, or longer. In some embodiments, the incubation time used for attaching streptavidin or biotinylated protein may be at least 10 minutes, at least 20 minutes, at least 30 minutes, at least 40 minutes, at least 50 minutes, or at least 60 minutes. In some embodiments, the incubation time used for attaching streptavidin or biotinylated protein may be at most 60 minutes, at most 50 minutes, at most 40 minutes, at most 30 minutes, at most 20 minutes, or at most 10 minutes. Those of skill in the art will recognize that the incubation time used for attaching streptavidin or biotinylated protein may have any value within this range, for example, about 34 minutes.

[0086] As yet another example, in embodiments of the disclosed methods where His-tagged proteins are immobilized to supported lipid bilayers using anchor lipid molecules comprising Ni-NTA (or other chelated metal ion) ligands, the mole percent of Ni-NTA-containing lipid

molecule used to form the bilayer may be varied in order to control the surface density of Ni-NTA ligands available for binding. The concentration of Ni-NTA-containing lipid molecules may range from as little as 1 mole percent to as much as 90 mole percent, or more. In some embodiments, the concentration of Ni-NTA-containing lipid molecules in the supported lipid bilayer may be at least 1 mole percent, at least 2.5 mole percent, at least 5 mole percent, at least 10 mole percent, at least 20 mole percent, at least 30 mole percent, at least 40 mole percent, at least 50 mole percent, at least 60 mole percent, at least 70 mole percent, at least 80 mole percent, or at least 90 mole percent. In some embodiments, the concentration of Ni-NTA-containing lipid molecules in the supported lipid bilayer may be at most 90 mole percent, at most 80 mole percent, at most 70 mole percent, at most 60 mole percent, at most 50 mole percent, at most 40 mole percent, at most 30 mole percent, at most 20 mole percent, at most 10 mole percent, at most 5 mole percent, at most 2.5 mole percent, or at most 1 mole percent. Those of skill in the art will recognize that the concentration of Ni-NTA-containing lipid molecules in the supported lipid bilayer may have any value within this range, for example, about 4.5 mole percent. Alternatively, the concentration and/or incubation time used for attaching His-tagged proteins (or other His-tagged biological entities) to the Ni-NTA groups in the lipid bilayer may be varied. The concentration of His-tagged protein (or other His-tagged biological entities) used for attachment may range from about 0.1 μM to about 10 μM, or more. In some embodiments, the concentration of His-tagged proteins (or other His-tagged biological entities) used may be at least 0.1 μM, at least 0.5 μM, at least 1 μM, at least 2 μM, at least 3 μM, at least 4 μM, at least 5 μM, at least 6 μM, at least 7 μM, at least 8 μM, at least 9 μM, or at least 10 μm. In some embodiments, the concentration of His-tagged proteins (or other His-tagged biological entities) used may be at most 10 μM, at most 9 μM, at most 8 μM, at most 7 μM, at most 6 μM, at most 5 μM, at most 4 μM, at most 3 μM, at most 2 μM, at most 1 μM, at most 0.5 μM, or at most 0.1 μM. Those of skill in the art will recognize that the concentration of u His-tagged proteins (or other His-tagged biological entities) used may have any value within this range, for example, about 7.5 μM. Expressed in terms of the amount of His-tagged proteins (or other His-tagged biological entities) used for attachment, the amount may range from about 1 nanogram to about 1,000 nanograms, or more. In some embodiment, the amount of His-tagged proteins (or other His-tagged biological entities) used for attachment may be at least 1 nanogram, at least 10 nanograms, at least 25 nanograms, at least 75 nanograms, at least 100 nanograms, at least 200 nanograms, at least 300 nanograms, at least 400 nanograms, at least 500 nanograms, at least 600 nanograms, at least 700 nanograms, at least 800 nanograms, at least 900 nanograms, or at least 1,000

nanograms. In some embodiments, the amount of His-tagged proteins (or other His-tagged biological entities) used for attachment may be at most 1,000 nanograms, at most 900 nanograms, at most 800 nanograms, at most 700 nanograms, at most 600 nanograms, at most 500 nanograms, at most 400 nanograms, at most 300 nanograms, at most 200 nanograms, at most 100 nanograms, at most 75 nanograms, at most 50 nanograms, at most 25 nanograms, at most 10 nanograms, or at most 1 nanogram. Those of skill in the art will recognize that the amount of His-tagged proteins (or other His-tagged biological entities) used for attachment may have any value within this range, for example, about 425 nanograms. The incubation time used for attaching His-tagged proteins (or other His-tagged biological entities) may range from about 10 minutes to about 60 minutes, or longer. In some embodiments, the incubation time used for attaching His-tagged proteins (or other His-tagged biological entities) may be at least 10 minutes, at least 20 minutes, at least 30 minutes, at least 40 minutes, at least 50 minutes, or at least 60 minutes. In some embodiments, the incubation time used for attaching His-tagged proteins (or other His-tagged biological entities) may be at most 60 minutes, at most 50 minutes, at most 40 minutes, at most 30 minutes, at most 20 minutes, or at most 10 minutes. Those of skill in the art will recognize that the incubation time used for attaching His-tagged proteins (or other His-tagged biological entities) may have any value within this range, for example, about 48 minutes.

Variation of SHG Signal with Surface Density of Immobilized Biological Entities

[0087] Surprisingly, the increase in SHG signal observed for increasing surface densities of immobilized, labeled biological molecules on the optical interface exceeded expectations based on equation (1) under some conditions. As illustrated in Example 1 below, an approximately 3.3-fold increase in the number of immobilized protein molecules (assuming saturation of the available binding sites on the surface by the labeled protein molecules) resulted in a dramatic increase in SHG signal intensity, *i.e.* a much larger increase than expected from the squared power law dependence of SHG signal on the number or surface density of immobilized proteins alone. This result is borne out by the data presented in Example 2 as well.

[0088] Further refinement of the protocols used for immobilization of labeled proteins or other biological entities may yield further increases in the SHG signal intensity (or other nonlinear optical signal) observed for increased surface density of the immobilized component. In some embodiments, a 2-fold increase of the concentration of anchor molecule used for immobilization (or the number or surface density of the immobilized biological

entity) may yield at least a 5x increase, at least a 10x increase, at least a 15x increase, or at least a 20x increase in the nonlinear optical signal detected. In some embodiments, a 2-fold increase of the concentration of anchor molecule used for immobilization (or the number or surface density of the immobilized biological entity) may yield at most a 20x increase, at most a 15x increase, at most a 10x increase, or at most a 5x increase in the nonlinear optical signal detected.

Devices and Kits

[0089] It will be apparent to those skilled in the art that the methods for immobilizing biological entities disclosed herein may be used in producing devices and kits for enabling non-linear optical measurements of conformation, orientation, or changes in conformation or orientation in biological molecules and other biological entities.

[0090] As one non-limiting example of devices disclosed herein, consider a device comprising: (a) a substrate, wherein the substrate further comprises a supported lipid bilayer; and (b) a biological entity, wherein the biological entity comprises an non-linear active label and is tethered to the supported lipid bilayer using a pair of affinity tags, and wherein one of the affinity tags is attached to the supported lipid bilayer and the other affinity tag is attached to the biological entity; and wherein the device is capable of producing a non-linear optical signal when exposed to excitation light.

[0091] A device of this type may be configured in a variety of different ways, for example, the substrate may be fabricated from a material selected from the group including, but not limited to, glass, fused-silica, a polymer, or any combination thereof. A variety of affinity tags may be used, including Ni-NTA (or other chelated metal ions) and poly-histidine tags, or biotin and streptavidin (or avidin, or neutravidin). In devices comprising the use of poly-histidine tags, the poly-histidine tag may be attached to the N-terminus of a protein or to the C-terminus of a protein, or at any other position in the protein's sequence that maintains protein function and also provides suitable exposure on the protein surface so that the poly-histidine tag is able to interact with Ni-NTA or other chelated metal ion ligands. As will be apparent to those skilled in the art, poly-histidine tags may comprise any suitable number of histidine residues, for example, something between 4 and 12 histidine residues, or about 9 histidine residues, or about 6 histidine residues. Another example of a chelated metal ion that may be used as a suitable ligand for binding poly-histidine tags is Co-CMA. Examples of non-linear optical signals that may be produced by the device when exposed to excitation light include second harmonic light, sum frequency light, and difference frequency light. A

variety of different biological entities may be utilized in such devices including, but not limited to, cells, proteins, peptides, receptors, enzymes, antibodies, DNA, RNA, biological molecules, oligonucleotides, small molecules, synthetic molecules, carbohydrates, or any combination thereof.

[0092] As one non-limiting example of kits disclosed herein, consider a kit comprising (a) a substrate; (b) a lipid suspension, wherein the lipid suspension is capable of forming a supported lipid bilayer on a surface of the substrate; and (c) affinity tagged reagents for tethering biological entities to the supported lipid bilayer.

[0093] Kits may be configured in a variety of different ways, for example, the device substrate may be fabricated from a material selected from the group including, but not limited to, glass, fused-silica, a polymer, or any combination thereof. A variety of affinity tagged reagents could be used in the kit, including Ni-NTA (or other chelated metal ion ligand) and poly-histidine tagged reagents, or biotinylated reagents along with streptavidin (or avidin, or neutravidin). The lipid suspension used for formation of supported lipid bilayers may include a variety of different phospholipids or other suitable lipids, for example, in some embodiments, the kits may include 1,2-dioleoyl-sn-glycero-3-phosphocholine and/or 1,2-dioleoyl-sn-glycero-3-[(N-(5-amino-1-carboxypentyl)iminodiacetic acid)succinyl] (nickel salt). It will be apparent to those of skill in the art that many other lipids and affinity tagged reagents may be used in kits of the present disclosure.

Example 1 - Ni-NTA Immobilization

[0094] The objective of this study was to demonstrate the use of His-tag chemistry for immobilizing labeled proteins (*i.e.* labeled with an SHG-active label) to substrate surfaces comprising the optical interface used in SHG measurements.

[0095] For the data shown in FIG. 3, 5μM DHFR enzyme labeled with either PyMPO-maleimide (Mal) or PyMPO-succinimidyl ester (SE) was incubated on a bilayer surface containing 10% Ni-NTA. Each protein was incubated for 60 minutes at room temperature in assay buffer containing 50mM NaPO4 pH 7.0. Unbound protein was removed by washing with assay buffer. The slide was then placed on an SHG instrument and each sample was scanned for SHG intensity. A well with no protein added was used as a control to establish the baseline SHG signal intensity for each well containing labeled protein.

[0096] FIG. 4 is an overlay of SHG data acquired using labeled protein bound to a lipid bilayer comprising 3% Ni-NTA (under slightly different incubation conditions) and that for the 10% Ni-NTA data to show the relative SHG intensity produced by each labeled protein

on their respective surfaces. The 10% NTA surfaces provided more than an order of magnitude improvement in the SHG signal for the labeled enzyme tested here.

Example 2 – Ni-NTA Immobilization

[0097] *Protein labeling protocol:* Stock His-tagged maltose binding protein (MBP) (1 mL at nominal 0.5 mg/mL) was buffer exchanged from 20mM Tris-HCL pH 8.0, 0.1M NaCl, 10% Glycerol into 0.1 M Na phosphate, pH 7.5 by passing over two of the 2 mL Zeba™ Spin Desalting Columns (Thermo Scientific) equilibrated per the manufacturer's instructions. Concentration and volume of the buffer exchanged material were determined by measuring absorbance on a NanoDrop Spectrophotometer (Thermo Scientific). PyMPO-NHS was weighed out and dissolved to 2mM in dry DMSO. PyMPO-NHS was added to the buffer exchanged MBP at 3.5:1 mole equivalents. The conjugation reaction was allowed to proceed in the dark at room temp, stirring gently, for 15 minutes. The reaction was terminated by buffer exchange back into the MBP storage buffer (20mM Tris-HCL pH 8.0, 0.1M NaCl, 10% Glycerol) over a fresh pair of Zeba™ Spin Desalting Columns. The resultant conjugate was centrifuged at 16K x g for 20 minutes at 4°C, and volume, concentration and degree of labeling was determined for the supernatant by measuring absorbance at 280 nm and 410 nm on the NanoDrop. Aliquots of the conjugate were snap frozen in liquid N_2 and stored at -80 °C. The resulting conjugate concentration was 9.74 x 10-6 M with a degree of labeling (DoL) of 2.4.

[0098] *Slide preparation:* A glass slide was cleaned by Piranha treatment (heating at 100 °C in 30% H2O2/70% con H2SO4 for 30 minutes). The slide was washed extensively in diH_2O, dried with N_2 gas, and a well-forming gasket was affixed.

[0099] *Bilayer preparation:* Small unilamellar lipid vesicle (SUV) solutions consisting of 3% DGS-NTA, Ni salt, or 10% DGS-NTA, Ni salt, at a stock concentration of 0.5 mg/mL were diluted to 0.1 mg/mL in 25 mM Tris-HCl, ph 7.2, 150 mM NaCl. 10 uL aliquots were then added to wells, and incubated at room temperature for 60 minutes to allow bilayer formation. Excess SUV were washed out with 10 x 20 uL of either DHFR Assay buffer (50mM Na phosphate pH 7.0, 100 uM NADPH) or MBP Assay buffer (20 mM Tris-HCl, pH 8.0, 150 mM NaCl, 0.05% Tween-20, 1 mM DTT), leaving 10 uL behind at the end of the wash step.

[00100] *Tethering of proteins:* MBP and DHFR conjugates were diluted to 5 uM in their respective assay buffers, and 10 uL was added to the appropriate wells, thereby resulting in a concentration of 2.5 uM in the wells. 10 uL of assay buffer was added to the bilayer-only

controls. Protein tethering was allowed to proceed for 1 hour at room temperature. During the tethering incubation, solutions of 2 mM lactose and 2 mM maltose were made up in MBP assay buffer. At the end of the tethering incubation, excess protein was washed out with 10 x 20 uL each of the appropriate assay buffer, leaving a volume of 10 uL in the wells, and the slide was mounted on the Artemis SHG System for scanning.

[00101] *Scanning:* The entire slide was line scanned to gather SHG data for determining the relative tethering efficiency of 3% vs 10% Ni-NTA surfaces. Well positions for 10% Ni-NTA tethered MBP were recorded and used to set up the MBP kinetic reads (3 wells total).

[00102] The chopper was placed 'in line' and operated at 120 Hz. The first objective was to show maltose-induced conformational change, using 10 uL buffer and 10 uL lactose injections as negative controls. For each injection, a volume of 10 uL was injected to give a total of 20 uL/well, and the volume was mixed by repetitively drawing up 10 uL volumes (4-5 times), then withdrawing 10 uL of liquid to leave 10 uL in the well. This same routine was followed for the maltose injection, but at the end, 10 uL was not removed, leaving 20 uL in the well. The assay was successful in showing that MBP only responded to maltose, not to lactose or buffer negative controls, but SHG signal appeared to be dropping with exposure time.

[00103] To differentiate dissociation of protein from photobleaching, the second MBP well was exposed for a few seconds (chopper in), then the beam was blocked, and the cycle was repeated to yield 7 short exposures over approximately 320 seconds. The signal appeared to drop even when the beam was blocked, indicating that some protein may be dissociating from the surface.

[00104] The conformation change evaluation was repeated, and again the MBP only responded to addition of maltose, not to the lactose or buffer negative controls. It also appeared that the slope of the line for the post-maltose injection was steeper than the pre-injection part of the trace.

[00105] The conformational change evaluation was again repeated using the last well. A few seconds after adding maltose, the beam was blocked for ~60 seconds before unblocking again to see if the signal continued to drop, which it appeared to do. The observed signal drop is most likely a combination of dissociation and photobleaching. It is not clear if the rate increased after conformational change was induced by maltose.

[00106] FIG. 5 shows a plot of SHG signal intensity data for PyMPO-labeled, His-tagged maltose binding protein (MBP) tethered to supported lipid bilayers doped with either 3% Ni-NTA-DGS or 10% Ni-NTA-DGS as described above. Despite some evidence for time-

dependent changes in signal that may be due to photobleaching and/or protein dissociation over time, dramatic improvement in SHG signal intensity was observed for His-tagged, PyMPO-labeled protein tethered to supported lipid bilayers prepared using the higher Ni-NTA concentration.

Example 3 – Protein Conformational Changes Detected & Resolved Site-Specifically

[00107] *Background:* In order to validate SHG as a broadly applicable biophysical technique to investigate protein structural motion, three model proteins were examined for studying ligand-induced conformational change: calmodulin (CaM), maltose binding protein (MBP), and Escherichia coli (E. coli) dihydrofolate reductase (DHFR).

[00108] MBP is a soluble, well-behaved protein in which the relationship between ligand binding, function, and conformational change has been extensively investigated by X-ray crystallography, NMR, and other biophysical techniques [8-15]. MBP belongs to a class known as periplasmic-binding proteins which are responsible for efficient uptake and catabolism of maltodextrins. Periplasmic-binding proteins share a two-domain structure linked by a flexible β-strand and are known to undergo large-scale motion from an open to a closed form upon binding maltose [16]. The transition from the open to closed form of MBP has also been exploited as a platform for developing biosensors for specific target compounds [17, 18].

[00109] CaM is a messenger protein that transduces calcium-generated signals by binding calcium ions [19]. CaM is implicated in numerous biological processes. The structural transition of CaM upon calcium ion binding has been extensively characterized by biochemical and biophysical techniques [20-24]. Calcium-free CaM adopts an extended, dumbbell structure with two similar lobes, each containing two calcium ion-binding sites. Binding of calcium ions changes the relative orientation of the helices flanking the calcium-binding loops, exposing a hydrophobic surface region that serves as a binding site for target proteins. Upon binding of a target protein, the two lobes of CaM collapse at the central helix to fold around the target peptide.

[00110] DHFR is a popular enzyme model for studying the relationship between conformational change and catalysis [25-27]. In cells, DHFR catalyzes the reduction of dihydrofolic acid to tetrahydrofolic acid with NADPH as an electron donor [28]. Tetrahydrofolate serves as cofactor in many reactions and is essential for purine and thymidylate biosynthesis, and thus cell growth, making DHFR a target for anticancer and antibacterial drugs [29]. During the catalytic cycle, DHFR converts between the closed and

occluded forms of the protein which involves large conformational changes in the Met20 loop [30, 31]. In the closed form, the Met20 loop protects the active site from the solvent by packing against the nicotinamide ring of NADPH, bringing it into close proximity to dihydrofolic acid. In the occluded form, the Met20 loop projects into the active site and sterically blocks the nicotinamide ring. The transition from the occluded to closed state is associated with the rate-determining step in the catalytic cycle [27].

[00111] In the work presented here, we demonstrate a broadly applicable method based on second-harmonic generation (SHG) to study protein conformational changes upon ligand binding, in real time and under physiological conditions. We demonstrate that tethering of proteins to a biomimetic lipid membrane using immobilized metal affinity chemistry allows for facile capture of labeled protein molecules that also retain their function as shown by an ability to undergo well- characterized conformational changes. We demonstrate that different conformational changes induced by binding different ligands to the same labeled protein produce different responses by SHG. We also validate our SHG findings by identifying the labeled sites using mass spectrometry (MS) and correlating the changes we observe with the motion at these sites upon ligand binding as seen in the x-ray crystal structures. The advantages of SHG technique on lipid bilayer are discussed within. This work was recently published in Moree, *et al.* (2015), "Protein Conformational Changes Are Detected and Resolved Site Specifically by Second-Harmonic Generation", Biophys. J. 109:806-815.

[00112] *Results:* Characterization of protein attachment to the supported lipid bilayer. Both CaM and MBP have previously been examined for structural transitions upon ligand binding using SHG [32, 33]. However, in those experiments protein immobilization on the surface was accomplished using aldehyde-derivatized glass slides to covalently couple the protein via amine-containing residues to the surface. While tethering the protein directly to the slide achieves the noncentrosymmetric distribution required for SHG, this method of attachment is far from ideal as proteins immobilized in this manner have been shown to unfold or lose secondary structure [34, 35]. Because the direct attachment of protein to derivatized glass surfaces very often does not result in tethered and functional protein, we developed a supported lipid bilayer (SLB) interface as an attachment platform for SHG. SLBs are biomimetic and they have been used extensively in many biochemical and cell biology experiments with minimal impact on protein structure and function [36, 37].

[00113] We began by characterizing the attachment of the proteins to our SLB surface. The SLB surface we employed has integrated immobilized metal affinity (Ni-NTA) chemistry to specifically tether the proteins to the bilayer in an oriented manner via a poly-histidine tag at

the N- or C-terminus. To test the specificity of this interaction, each protein was incubated on the bilayer in the presence or absence of imidazole, a competitive inhibitor of His-tagged protein binding. As can be seen in Fig. 6A, incubation of the SH-functionalized proteins in the absence of imidazole results in a large increase in the SHG signal compared to the controls (addition of the unlabeled proteins or just the bilayer alone). When labeled protein is incubated in the presence of imidazole, SHG signal levels are reduced to less than 10% of the original signal or to background levels, i.e. to those of bilayer alone. Taken together, these results show that the SHG signal observed arises specifically from the dye-labeled protein bound via the His-tag-Ni-NTA linkage.

[00114] Next, we investigated the stability of the protein tethered to the SLB surface. Although the poly-histidine tag allows the protein to be captured and oriented in a specific manner on the SLB surface, the affinity of the 6x-His tag for Ni-NTA is only in the high nanomolar to low micromolar range (0.1-1μM) [38]. Given this range of affinities, we wanted to characterize the kinetics of protein loss from the SLB surface to the bulk solution after washout of the unbound protein fraction, as loss of protein due to unbinding from the surface could impact the measured change in SHG intensity over the time-course of our experiments. Protein was incubated overnight at 4°C, as it has been reported that the stability of poly-histidine tagged proteins on bilayers is greatly increased by longer incubation period [39]. Following washout of unbound protein, the SHG signal for each protein was monitored over the course of ~ 1 hour. FIG. 6B shows that after washout the SHG signal is nearly constant over one hour, with losses of 3% observed for DHFR and 16% for MBP, demonstrating minimal dissociation of protein from the surface over this time frame. The stability of the protein attachment to the bilayer provides confidence that signal changes observed during an experiment, which typically occur over seconds to a few minutes, are the result of conformational change and not protein dissociation from the surface. The stability of our system also enables the monitoring of relatively slow processes on the order of tens of minutes.

[00115] To further characterize our system, we explored the amount of protein required for producing reliable SHG signals on the bilayer surface. In these experiments, 100 ng of each of the model proteins was incubated on the bilayer for 1 hour, followed by buffer washout of excess protein. For each protein, signal of at least two-fold over background is observed (FIG. 6C). Finally, we measured the amount of the lysine-labeled MBP and DHFR proteins tethered to the membrane after washout with buffer. In order to do so, we tethered the proteins to the SLB, washed out the unbound protein with buffer, and then solubilized both

the protein and the bilayer with detergent (Supplementary section). The SHG label is also fluorescent and its signal intensity was measured by fluorimetry and compared to a standard curve of the same labeled proteins. At the incubation concentrations in the experiments described here, lysine-labeled MBP (pH 8.3 conjugation) and DHFR are tethered to the bilayer surface at densities of $4.9 \pm 0.7 \times 10^{12}$ molecules/cm^2 and $2.8 \pm 0.1 \times 10^{12}$ molecules/cm^2, respectively. Taken together, the data characterizing our SLB surface demonstrate that SHG-labeled, poly-histidine tagged proteins are specifically and stably attached to the bilayer surface via metal chelation, that an SHG signal over background can be generated from bulk incubation of as little as 100 ng of labeled protein, and that the measured SHG signals are generated by a monolayer or less of molecules given the dimensions of the proteins and their theoretical close-packed densities.

[00116] *MBP and CaM Proteins:* To explore the ability of our SHG bilayer system to detect and measure conformational changes of a protein, we began by testing the system on CaM and MBP, two proteins previously studied by SHG [32, 33]. First, we tethered labeled CaM to the SLB surface and monitored the change in SHG intensity upon addition of the calmodulin binding peptide (CBP) in the presence or absence of calcium-containing buffers. As seen in FIG. 7A, the addition of 2 μM CBP in the presence of a calcium-containing buffer resulted in a positive change in SHG signal of M = 18.1%, (N=3, SEM ± 0.6) whereas buffer injection resulted in a signal change of M = 0.1% (N=9, SEM ± 0.4). When calcium is omitted from the buffer, addition of the peptide alone results in M = 3.1%, (N=3, SEM ± 1.6) change in SHG intensity, essentially no change (FIG. 7B). As calcium-free calmodulin does not adopt a conformation capable of binding to peptide, these results confirm that the change observed upon peptide addition in the presence of calcium is due to the conformational change induced by peptide binding. Next, we evaluated the effect of adding calcium ions. When buffer containing 1 mM $CaCl_2$ is injected into the system, a decrease in signal of M = -12.6% (N=3, SEM ± 1.4) resulted (FIG. 7C). Peptide was then added directly to these samples two minutes after calcium addition, producing a positive signal change of M = 8.7% (N=3, SEM ± 0.4). The magnitude of signal changes for each of these experiments is shown in FIG. 7D. As the magnitude of the SHG signal is proportional to the net, average orientation of the dye label relative to the surface normal, the different magnitudes of SHG signal change upon binding CBP and calcium to unbound CaM confirm that these ligands bind to specific and different conformations of the protein. SHG signal changes can occur in either the positive or negative direction relative to baseline depending on whether the net,

average orientation of the probe moves closer to or further away from the surface normal, respectively.

[00117] We next sought to determine which residues were modified with our amine reactive dye. Mass spectrometry of labeled CaM revealed complete labeling at K115 and less than complete modification at K13 and K94. As the degree of labeling for CaM is 1.0 (dye:protein ratio), determined by measuring the UV-Vis spectrum, most of the signal is likely due to labeling at K115. As can be seen from the overlay of the crystal structures of the apo, Ca^{2+}-bound, and CBP-bound CaM in FIG. 7E, all three residues undergo large structural changes upon binding both calcium and CBP. Taken together, the data demonstrate the detection of conformational changes associated with both calcium and CBP binding to calmodulin using SHG. Moreover, the peptide- and Ca^{2+}-induced conformational changes are clearly different in both magnitude and directionality, illustrating SHG's ability to discriminate the different conformations the protein adopts upon binding different ligands.

[00118] We also performed a similar set of experiments with MBP. First, we monitored the SHG intensity of MBP labeled at pH 8.3 upon addition of buffer, lactose, or maltose. As can be seen in the real-time trace of the SHG signal, the addition of 2mM maltose resulted in an instantaneous decrease of M = -33.8% (N=4, SEM ± 1.0), whereas the addition of either buffer or 2mM lactose resulted in a negligible change of M = 0.12% (N=4, SEM ± 0.61) or M = 0.44% (N=4, SEM ± 0.79) respectively (FIG. 8A). The MBP system offers an excellent control in lactose, a stereoisomer of maltose that does not bind to MBP. Because the addition of both 2 mM lactose and buffer alone result in negligible changes in SHG intensity, the change in SHG intensity upon maltose addition is specific to ligand-induced conformational change upon binding.

[00119] Mass spectrometry analysis of MBP revealed that it is heterogeneously labeled at nine lysine residues present in the sequence, although residues K15, K88, and K362 represent approximately 90% of the total population of modified peptides. The degree of labeling for MBP is 1.3, confirming that more than one residue is labeled. We aligned the crystal structures of the apo and maltose-bound MBP and compared the positions of the labeled residues in these two structures. As can be seen in FIG. 8D, the side chains of the labeled residues show significant orientational differences, providing further validation that the observed change in SHG intensity is the result of ligand-induced binding of maltose to MBP.

[00120] As MBP demonstrated a high degree of lysine modifications, we modified our labeling conditions to explore whether we could target specific lysines for labeling. Labeling MBP at pH 7.5 rather than pH 8.3 significantly increased the overall abundance of the K15

modification with a corresponding decrease in the modification at K88; 70% of the peptides detected by MS show labeling at K15 rather than K88. The converse trend, preference at K88 over K15, was observed when the experimental conditions changed to pH 8.3. The degree of labeling of the conjugate labeled at pH 7.5 is 1.3, which also suggests that the protein is primarily labeled at K15. This example shows that by varying the conditions of the conjugation reaction, one can bias the distribution of labeled lysines to favor one among multiple ones, by exploiting the differences in the residue's microenvironment and pKa, for example. Based on inspection of the crystal structures, we hypothesized that when MBP is primarily labeled at K15 rather than K88, this could alter the directionality of SHG signal change upon ligand addition relative to the reverse case, since K15 and K88 appear to rotate towards and away from the surface normal, respectively, assuming the protein is oriented with its N-terminus facing the bilayer. As can be seen in FIG. 8B, addition of 2mM maltose to pH 7.5 labeled MBP results in an increase in the SHG intensity of M = 27.4% (N=3, SEM ± 0.61). Consistent with previous results, the addition of lactose and buffer alone had no effect.

[00121] *Dihydrofolate reductase:* As a final demonstration of the technique, we studied E. coli DHFR, a protein previously uncharacterized by SHG. In particular, we focused on the protein's response to two important pharmaceutical inhibitors: methotrexate (MTX) and trimethoprim (TMP)[29]. For these studies, we chose two approaches to label the protein: native lysine residues and an engineered, unique cysteine at residue 20. As seen in FIG. 9A, the addition of 1 μM MTX to the amine labeled DHFR resulted in a rapid decrease in SHG signal of M = -60.2% (N=4, SEM ± 1.26) compared to M = -2.27% (N=8, SEM ± 0.48) for the buffer control. As a control to show that the SHG signal change arises from the change in conformation upon the binding of MTX and not loss of protein from the surface, a competition experiment was carried out with the antibiotic TMP. Both MTX and TMP bind to the folate pocket on DHFR with high affinity, so addition of excess TMP should inhibit the change in SHG intensity upon MTX addition. We began by exploring whether TMP addition by itself would result in a conformational change in DHFR. As can be seen in FIG. 9B, the addition of 100μM TMP resulted in a decrease in SHG intensity of M = -33.9% (N=4, SEM ± 5.31). Subsequent addition of 1 μM MTX resulted in a decrease of M = -3.48% (N=4, SEM ± 1.31) in SHG signal. This small change in SHG intensity is not significantly different than the buffer control, and the absence of signal change in this competition experiment is expected as both MTX and TMP compete for the same binding site. These results are summarized in FIG. 9C. MS analysis revealed that three residues, K76, K106, and K109, are modified by the

amine-reactive SHG dye, with the modification at K76 being nearly complete. The degree of labeling of the amine-labeled DHFR conjugate is 1.1, suggesting that labeled K76 is the primary contributor to the observed signal. As seen in FIG. 9D in an overlay of the x-ray structures of the apo and MTX-bound DHFR holoenzyme there is relatively little motion at sites K106 and K109 but significant reorientation at site K76, corroborating our SHG measurements and the MS analysis.

[00122] We also performed the same series of experiments on DHFR labeled specifically at a single-site engineered cysteine (M20C). Complete labeling of the cysteine residue was confirmed by mass spectrometry and the degree of labeling was 1.0 indicating that the labeling was site-specific. The ΔCys M20C construct maintained the wild-type enzymatic activity. As seen in FIG. 10A, the trends are similar to those seen with amine-labeled DHFR, although the magnitude of the observed change is different. Addition of MTX to cysteine-labeled DHFR on the bilayer resulted in a large change in the SHG intensity of M = -75.6% (N=3, SEM ± 1.18) compared to M = -1.3% (N=4, SEM ± 0.36) for buffer alone. Surprisingly, addition of TMP alone produces an even larger decrease in SHG intensity of M = -84.7% (N=3, SEM ± 0.57) and, as with amine-labeled DHFR, addition of 1μM MTX in the presence of TMP resulted in an insignificant change in SHG intensity of M = -1.9% (N=3, SEM ± 1.02) (FIG. 10B), which can be rationalized by a relatively long residence time for TMP bound to DHFR {Carroll, 2012 #731}. These results are summarized in FIG. 10C.

[00123] *Discussion:* In the work described here, we demonstrate a broadly applicable and sensitive approach using SHG for detecting and resolving ligand-induced protein conformational changes using three different examples (CaM, MBP, and E. coli DHFR) proteins. This approach is based on using labeled proteins tethered to a supported lipid bilayer membrane. While most proteins are not intrinsically SH-active, proteins can be easily made so by standard amine- and thiol-reactive chemistries. We identified the labeled sites by mass spectrometry which, when combined with the available x-ray crystal structures, allowed us to inspect and confirm the structural motions that we observe by SHG to the motion observed at the modified residues in both the apo and bound structures for all three proteins.

[00124] In addition to providing direct evidence that the changes in SHG signal upon ligand binding result from motion at specific labeled residues, the MS analysis also provided indirect support for the orientation of the protein on the bilayer. Because the intensity of the SHG signal is directly dependent on the net, average orientation, the motion at the predominantly labeled residues can be inferred using the direction of the SHG signal change. For example, because the signal change in DHFR upon MTX addition decreased, we would

expect that the K76 side chain would likely move away from the surface normal. The protein is tethered to the surface through the N-terminal poly-histidine tag and a large rotation of the K76 side chain away from the normal upon MTX addition is easily seen by inspection of the crystal structures. Only small motions are observed for the other modified residues, K106 and K109, suggesting that K76 contributes the majority of the motion we observe in amine-labeled DHFR samples.

[00125] We also probed the ability to target specific label sites by changing the pH of the conjugation reaction. At lower pH, the reduction of the K88 modification and subsequent enrichment of the K15 modification under these conditions resulted in the SHG response of MBP binding to maltose switching directionality, from a decrease in intensity relative to baseline for protein labeled at pH 8.3, to an increase in intensity for protein labeled at pH 7.5. As there are no other differences in the MS analysis between the conjugates labeled at these two pH's, this change in signal directionality is most likely due to the difference in the direction of movement between residues K15 and K88. The motion of the K88 residue upon MBP binding should cause a decrease in the SHG intensity with the protein tethered to the surface through the N-terminal poly-histidine tag, consistent with our observations (FIG. 8A). In contrast, with labeling predominantly at K15, we would expect an increase in SHG signal intensity, which is also consistent with the SHG results (FIG. 8B).

[00126] In addition to SHG's sensitivity, the technique offers a number of advantages over traditional methods for probing conformational change, one of which is the relative ease of performing experiments, as no a priori structural knowledge or engineering of the protein is required. The only requirements for sample preparation are the incorporation of a poly-histidine tag and the labeling of the target protein to make it SH-active. Multiple approaches can be taken to label proteins as we have demonstrated here, including labeling of lysines through amine-reactive chemistry, site specific labeling of native or engineered cysteines through thiol-reactive chemistry, and preferentially favoring specific residues by changing the conjugation conditions. Moreover, relatively small amounts of protein are required for each experiment (100's of ng).

[00127] A highly sensitive and generally applicable structural technique, like the SHG-based approach described here, can offer great utility in many facets of research, such as probing the functional and implications of structural rearrangement in a specific region of a protein due to ligand/drug/protein-protein interactions, assessing protein viability and stability, protein identification, optimization of formulation or effect of conditions, and mutational screening.

[00128] Using our approach, conformational changes that occur with binding or activity can readily be probed under a variety of experimental conditions such as different buffers, the presence of diverse ligands (e.g., peptides, cofactors), and across a wide range of protein or ligand concentrations. Furthermore, the approach offers the opportunity to draw correlations between the SHG structural measurements and data obtained from in vivo and pharmacological experiments. Here we show that E. coli DHFR generated different SHG signals when the enzyme was bound to two different pharmaceutical inhibitors. The SHG signals are very reproducible, and the difference between the two signals – and thus conformations - are easily distinguished. Thus the compounds produce distinct conformational changes upon binding to the protein. Knowing that the inhibition constant (Ki) between MTX and TMP is ~100 times (in favor of MTX), one might be able to establish a structure-activity relationship by evaluating the Ki value against the magnitude of the SHG signal change (e.g., from apo to bound forms). Once such an SAR is established, the SHG platform could offer a more convenient and efficient way to screen for potential drug candidate over the current activity and kinetic-based assays.

[00129] Another advantage of SHG is that there are no restrictions on the size or type of protein for study by SHG; large molecular weight proteins, protein complexes, and intrinsically disordered proteins can all be studied. Likewise, the technique is amenable to all types of ligands, from chemical fragments to small molecules to larger proteins for probing small molecule and protein-protein interactions since the technique does not depend on mass accumulation to produce a signal. The modest protein requirement for SHG measurements should allow large-scale structure-based screens not currently possible using other biophysical methods, which generally require much higher amounts of protein. In addition, the relatively low protein concentration requirement indicates that the technique lends itself well to study proteins that are not soluble or prone to aggregation at the higher concentrations required for techniques such as NMR and X-ray crystallography. Unlike both X-ray crystallography and NMR studies, which are time and resource-intensive, SHG requires as little as 100 ng of labeled protein per sample, making the technique amenable to high-throughput structural screening of compound libraries with relatively little protein consumption. The technique's attributes suggests a number of other applications as well, such as serial additions of different ligands in permuted order to determine mutual binding dependencies.

[00130] In summary, our data demonstrate that the SHG-based method presented here sensitively detects ligand-induced conformational changes that range in magnitude from the

relatively small rotation of an amino acid side chain to the global motion of protein domains. The SHG measurements are strengthened by MS analysis to identify the labeled residues and corroborated by inspection of the crystal structures between the unbound and bound forms of the protein to confirm that motion occurs at the labeled sites. Enabled by the biomimetic SLBs as a two-dimensional platform for tethering and orienting proteins, SHG offers a straightforward means to provide new information about structure, function and activity on a broad range of proteins and under diverse conditions.

[00131] *Methods - Lipids and SUV Preparation:* 1,2-Dioleoyl-sn-glycero-3-phosphocholine (DOPC) and 1,2-dioleoyl-sn-glycero-3-([N-(5-amino-1-carboxypentyl)iminodiacetic acid]succinyl) (DOGS-NTA) were obtained from Avanti Polar Lipids (Alabaster, AL). Texas Red® 1,2-dihexadecanoyl-sn-glycero-3-phosphoethanolamine (Texas Red® DHPE) was obtained from Life Technologies (Grand Island, NY).

[00132] *Methods – Stock Solutions:* Stock solutions of DOPC, DOGS-NTA, and DHPE Texas Red lipids were made up in chloroform and mixed to give the appropriate molar ratio. The mixture was placed in a Roto-Vap (Buchi Rotovapor R-210) and chloroform was removed by evaporation under vacuum for 2 h. Any residual chloroform was removed by blowing dry nitrogen gas over the cake for 5 min. The dried lipids were resuspended in diH2O at a total lipid concentration of 0.5mg/mL. SUV were prepared using a Sonic Dismembator Ultrasonic Processor (Fisher Scientific) at 25% amplitude for 90 seconds. The SUV prep was then centrifuged for 30 min at 16,873xg and the supernatants stored at 4 °C until use.

[00133] *Methods - Proteins and Labeling:* N-terminal poly-histidine tagged MBP was purchased from AtGen Co, Ltd (Seongnam-si, Gyeonggi-do, South Korea). N-terminal poly-histidine tagged human calmodulin was obtained from EMD Millipore (Billerica, Massachusetts). The N-terminus His-tag (8 His) ecDHFR variants were constructed using the Stratagene QuikChange site-directed mutagenesis kit and the wild-type ecDHFR template as described.(ref: Cameron CE, Benkovic SJ (1997) Evidence for a Functional Role of the Dynamics of Glycine-121 of Escherichia coli Dihydrofolate Reductase Obtained from Kinetic Analysis of a Site-Directed Mutant. Biochemistry 36(50):15792-15800) For the His-tagged M20C variant, the two native cysteines (C85 and C152) in the wild-type enzyme were mutated to Ala and Ser, respectively, to generate a ΔCys ecDHFR as described elsewhere (ref: Liu CT, et al. (2014) Probing the Electrostatics of Active Site Microenvironments along the Catalytic Cycle for Escherichia coli Dihydrofolate Reductase. J Am Chem Soc 136(29):10349-10360). The choice of amino acid substitution (C85A/C152S) was shown to

have no impact on the enzymatic activity. Selective incorporation of cysteine was achieved through subsequent mutations using the primer: 5'- GGC ATG GAA AAC GCC TGT CCA TGG AAC CTG -3'. Plasmid construction, protein expression, and purification of mutant DHFRs were performed according to the published protocol (cite: the Cameron & Benkovic 1997 paper above). The purified His-tag E. coli DHFR and its single-cysteine M20C derivative were found to have enzyme activity comparable to that of the WT enzyme. The His-tag WT enzyme, His-tag M20C, and non-His-tag WT E coli DHFR yielded hydride transfer rates of 205±20 s-1, 180±10 s-1, and 220 s-1 at pH 7 and 25 °C (under standard kinetic condition described in ref [28].

[00134] The SH-active dyes PyMPO-SE and PyMPO-maleimide were synthesized by ChemShuttle (Wuxi City, China). The dye was conjugated to each protein using standard coupling techniques for either amine or thiol reactive dyes. Unless otherwise indicated, labeling reactions for the amine reactive dye were carried out at pH 8.3. Thiol-reactive dye reactions were carried out at pH 7.0. The labeled protein was separated from the free dye with Zeba Spin Desalting columns with a 7K MWCO (Thermo Fisher, Rockford, IL). The UV-Vis spectra of each conjugated was measured and the degree of labeling (dye:protein stoichiometry) was determined using the known extinction coefficients of the proteins and the dye. The identification and analysis of the dye-modified residues by Liquid Chromatography/Mass spectrometry were performed by Martin-Protein (Princeton, NJ).

[00135] *Methods - Sample Preparation:* Glass slides (Fisher) were cleaned in Piranha (30% H2O2, 70% H2SO4) at 100□C for 20 minutes. After cooling, the slides were washed five times with deionized water and dried with nitrogen gas. A custom 2mm thick silicone gasket template with adhesive backing (Arrowleaf Research, Bend, Oregon, USA) was applied to cleaned slides. Each silicone gasket template defined 16 wells, each with a total volume of ~14 μL. The spacing and diameter of the wells is based on the standard 384-well plate format. SUV's were incubated with 1 mM $NiCl_2$ (Sigma, St. Louis, MO) for 30 minutes, diluted five-fold in buffer, and added to each well. After bilayer formation, wells were washed with buffer to remove unbound SUVs and imaged by fluorescence microscopy to determine that the bilayer was uniform across the surface[40]. Protein was then added to the wells at the desired concentration and allowed to incubate for a minimum of an hour. Excess protein was removed by additional washes after incubation.

[00136] Each protein was screened to determine an optimized binding buffer for bilayer attachment and SHG signal production. For MBP, the optimized buffer is 20 mM Tris pH 8.0, 150 mM NaCl, 0.05% Tween-20, and 1 mM DTT. For CaM, the optimized buffer is 25

mM MOPS pH 7, 150 mM KCl, 2 mM $MgCl_2$ (with or without 2 mM $CaCl_2$). For DHFR, the optimized buffer is 50 mM sodium phosphate, pH 7.0 with 100 µM NADPH (Sigma). For conformational change experiments, 9 µM MBP, 2 µM CaM, or 4µM DHFR was incubated in each well for a minimum of 1 hour. The stability experiments were carried out after overnight incubation in the wells at 4°C. For the specificity experiments, each protein was incubated in 25 mM Tris pH 7.2 and 150 mM NaCl, with or without 300 mM imidazole. Excess protein and imidazole was removed with by washing with 25 mM Tris pH 7.2, 150 mM NaCl prior to SHG data acquisition.

[00137] *Methods - SHG Instrumentation and Experiments:* Our instrument comprises a mode-locked Ti:Sapphire oscillator which provides the fundamental beam necessary to generate the second-harmonic signal (high peak power). For these experiments, we used a Mira 900 Ti:Sapphire ultrafast oscillator (Coherent Inc., Santa Clara, CA, USA) pumped by a Millenia V DPSS laser (Spectra-Physics Corp., Santa Clara, CA, USA). The fundamental was passed through a half-wave plate to select p-polarization (used for all the experiments described here), and focused into a Dove prism for total internal reflection (TIR) to a spot size of ~50 um. The second harmonic light was collected by a lens, separated from the fundamental using a dichroic mirror and wavelength filters, and directed into a PMT module with a built-in pre-amplifier for photon counting (Hamamatsu, Bridgewater, NJ, USA). A custom electronics board was used to digitize the signal and the data was sent to a computer running customized control and data collection software (Labview, National Instruments Corp. Austin, TX, USA).

[00138] For these experiments, the microscope slide with protein was coupled to a prism using BK7 index matching fluid (Cargille, Cedar Grove, NJ, USA) and the prism itself secured onto a 1-D translation stage capable of 10 µm randomly-addressable precision (Renishaw, Parker-Hannifin Corp, Rohnert Park , CA, USA).

[00139] Ligand addition was carried out while SHG signal was monitored in real time. Once baseline signal was established, buffer was injected into the well as a control. After 5-10 seconds to to assess how the buffer injection changed the signal, the compound of interest was injected into the well to the desired final concentration. SHG signal was monitored over several minutes after injection.

[00140] *Methods - SHG Quantification:* To calculate the percent change, the SHG intensity measured just prior to ligand injection (T_0) was subtracted from the SHG intensity at equilibrium (T_{eq}) and then normalized by T_0 according to the following equation: $SHG\% = (I_{SHG}@T_{eq} - I_{SHG}@T_0)/I_{SHG}@T_0$. The T_{eq} for each ligand was experimentally determined but

in most cases equilibrium was achieved in less than one minute. In addition, all experiments included a control buffer injection that was used to determine the threshold for SHG intensity change and was calculated in a similar manner.

Changes in SHG signal separated from the average buffer shift by more than three times the standard deviation of the buffer shift are considered to indicate a change in the angle of the dye and therefore the conformation of the protein at the labeled residue(s).

[00141] *Supplemental Methods - Quantification of the Surface Density of Protein Molecules:* Four wells each of MBP and DHFR were incubated in wells containing supported lipid bilayer at 4 uM in their respective buffers. After 1 hour, wells were washed 5 x 20 µL with the appropriate buffer, and SHG signal was measured to confirm binding. A 10 µl aliquot of PBS/LDAO was used to wash the first well and this was carried forward into three other wells so that protein was collected from a total of 4 replicate wells. Five more 10 µl aliquots of PBS/LDAO were used to wash out the wells in the same manner, so that in total 6 x 10 µl aliquots were used to wash out the 4 wells. Four wells were used to increase the fluorescence signal-to-noise and to average over separate wells. The wash was collected and monitored for PyMPO fluorescence on a Horiba Jobin Yvon Fluorolog F-1000 fluorimeter in a 384-well plate. PyMPO was excited at 415 nm and emission was collected from 520 to 620 nm. Standard curves for each labeled protein were generated (FIGS. 11A-C) to calculate the concentration of protein in the samples from the slides and therefore to determine the number of molecules tethered to the surface in one well.

[00142] *References:*

[00143] 1. Goodey, N.M. and S.J. Benkovic, Allosteric regulation and catalysis emerge via a common route. Nat. Chem. Biol., 2008. 4(8): p. 474-82.

[00144] 2. Goh, C.S., D. Milburn, and M. Gerstein, Conformational changes associated with protein-protein interactions. Curr. Opin. Struct. Biol., 2004. 14(1): p. 104-9.

[00145] 3. Kull, F.J. and S.A. Endow, Force generation by kinesin and myosin cytoskeletal motor proteins. J Cell Sci., 2013. 126(Pt 1): p. 9-19.

[00146] 4. Tompa, P., Intrinsically disordered proteins: a 10-year recap. Trends Biochem. Sci., 2012. 37(12): p. 509-16.

[00147] 5. Heinz, T.F., H.W.K. Tom, and Y.R. Shen, Determination of molecular orientation of monolayer adsorbates by optical second-harmonic generation. Physical Review A, 1983. 28(3): p. 1883-1885.

[00148] 6. Zhuang, X., et al., Mapping molecular orientation and conformation at interfaces by surface nonlinear optics. Physical Review B, 1999. 59(19): p. 12632-12640.

[00149] 7. Salafsky, J.S., 'SHG-labels' for detection of molecules by second harmonic generation. Chemical Physics Letters, 2001. 342(5-6): p. 485-491.

[00150] 8. Bucher, D., B.J. Grant, and J.A. McCammon, Induced fit or conformational selection? The role of the semi-closed state in the maltose binding protein. Biochemistry, 2011. 50(48): p. 10530-9.

[00151] 9. Evenas, J., et al., Ligand-induced structural changes to maltodextrin-binding protein as studied by solution NMR spectroscopy. J Mol. Biol., 2001. 309(4): p. 961-74.

[00152] 10. Kondo, H.X., et al., Free-energy landscapes of protein domain movements upon ligand binding. J Phys. Chem. B, 2011. 115(23): p. 7629-36.

[00153] 11. Seo, M.H., et al., Protein conformational dynamics dictate the binding affinity for a ligand. Nat. Commun., 2014. 5: p. 3724.

[00154] 12. Staii, C., D.W. Wood, and G. Scoles, Ligand-induced structural changes in maltose binding proteins measured by atomic force microscopy. Nano Lett., 2008. 8(8): p. 2503-9.

[00155] 13. Millet, O., R.P. Hudson, and L.E. Kay, The energetic cost of domain reorientation in maltose-binding protein as studied by NMR and fluorescence spectroscopy. Proc. Natl. Acad. Sci. USA, 2003. 100(22): p. 12700-5.

[00156] 14. Duan, X., et al., Crystal structures of the maltodextrin/maltose-binding protein complexed with reduced oligosaccharides: flexibility of tertiary structure and ligand binding. J Mol. Biol., 2001. 306(5): p. 1115-26.

[00157] 15. Spurlino, J.C., G.Y. Lu, and F.A. Quiocho, The 2.3-A resolution structure of the maltose- or maltodextrin-binding protein, a primary receptor of bacterial active transport and chemotaxis. J Biol. Chem., 1991. 266(8): p. 5202-19.

[00158] 16. Quiocho, F.A. and P.S. Ledvina, Atomic structure and specificity of bacterial periplasmic receptors for active transport and chemotaxis: variation of common themes. Mol. Microbiol., 1996. 20(1): p. 17-25.

[00159] 17. Medintz, I.L. and J.R. Deschamps, Maltose-binding protein: a versatile platform for prototyping biosensing. Curr. Opin. Biotechnol., 2006. 17(1): p. 17-27.

[00160] 18. Dwyer, M.A. and H.W. Hellinga, Periplasmic binding proteins: a versatile superfamily for protein engineering. Curr. Opin. Struct. Biol., 2004. 14(4): p. 495-504.

[00161] 19. Chin, D. and A.R. Means, Calmodulin: a prototypical calcium sensor. Trends Cell Biol., 2000. 10(8): p. 322-8.

[00162] 20. Kursula, P., Crystallographic snapshots of initial steps in the collapse of the calmodulin central helix. Acta Crystallogr. D Biol. Crystallogr., 2014. 70(Pt 1): p. 24-30.

[00163] 21. Grabarek, Z., Structure of a trapped intermediate of calmodulin: calcium regulation of EF-hand proteins from a new perspective. J Mol. Biol., 2005. 346(5): p. 1351-66.

[00164] 22. Marlow, M.S., et al., The role of conformational entropy in molecular recognition by calmodulin. Nat. Chem. Biol., 2010. 6(5): p. 352-8.

[00165] 23. O'Donnell, S.E., et al., Thermodynamics and conformational change governing domain-domain interactions of calmodulin. Methods Enzymol., 2009. 466: p. 503-26.

[00166] 24. Villarroel, A., et al., The ever changing moods of calmodulin: how structural plasticity entails transductional adaptability. J Mol. Biol., 2014. 426(15): p. 2717-35.

[00167] 25. Arora, K. and C.L. Brooks, 3rd, Multiple intermediates, diverse conformations, and cooperative conformational changes underlie the catalytic hydride transfer reaction of dihydrofolate reductase. Top. Curr. Chem., 2013. 337: p. 165-87.

[00168] 26. Hammes-Schiffer, S. and S.J. Benkovic, Relating protein motion to catalysis. Annu. Rev. Biochem., 2006. 75: p. 519-41.

[00169] 27. Schnell, J.R., H.J. Dyson, and P.E. Wright, Structure, dynamics, and catalytic function of dihydrofolate reductase. Annu. Rev. Biophys. Biomol. Struct., 2004. 33: p. 119-40.

[00170] 28. Fierke, C.A., K.A. Johnson, and S.J. Benkovic, Construction and evaluation of the kinetic scheme associated with dihydrofolate reductase from Escherichia coli. Biochemistry, 1987. 26(13): p. 4085-92.

[00171] 29. Schweitzer, B.I., A.P. Dicker, and J.R. Bertino, Dihydrofolate reductase as a therapeutic target. FASEB J, 1990. 4(8): p. 2441-52.

[00172] 30. Sawaya, M.R. and J. Kraut, Loop and subdomain movements in the mechanism of Escherichia coli dihydrofolate reductase: crystallographic evidence. Biochemistry, 1997. 36(3): p. 586-603.

[00173] 31. Venkitakrishnan, R.P., et al., Conformational changes in the active site loops of dihydrofolate reductase during the catalytic cycle. Biochemistry, 2004. 43(51): p. 16046-55.

[00174] 32. Salafsky, J.S., Detection of protein conformational change by optical second-harmonic generation. J Chem. Phys., 2006. 125(7): p. 074701.

[00175] 33. Salafsky, J.S., Second-harmonic generation as a probe of conformational change in molecules. Chemical Physics Letters, 2003. 381(5-6): p. 705-709.

[00176] 34. Menaa, B., et al., Favourable influence of hydrophobic surfaces on protein structure in porous organically-modified silica glasses. Biomaterials, 2008. 29(18): p. 2710-8.

[00177] 35. Menaa, B., et al., Protein adsorption onto organically modified silica glass leads to a different structure than sol-gel encapsulation. Biophys. J, 2008. 95(8): p. L51-3.

[00178] 36. Manz, B.N., et al., T-cell triggering thresholds are modulated by the number of antigen within individual T-cell receptor clusters. Proceedings of the National Academy of Sciences, 2011. 108(22): p. 9089-9094.

[00179] 37. Dustin, M.L. and J.T. Groves, Receptor Signaling Clusters in the Immune Synapse. Annual Review of Biophysics, 2012. 41(1): p. 543-556.

[00180] 38. Block, H., et al., Immobilized-metal affinity chromatography (IMAC): a review. Methods Enzymol., 2009. 463: p. 439-73.

[00181] 39. Nye, J.A. and J.T. Groves, Kinetic control of histidine-tagged protein surface density on supported lipid bilayers. Langmuir, 2008. 24(8): p. 4145-9.

[00182] 40. Nye, J.A. and J.T. Groves, Kinetic Control of Histidine-Tagged Protein Surface Density on Supported Lipid Bilayers. Langmuir, 2008. 24(8): p. 4145-4149.

[00183] While preferred embodiments of the present disclosure have been shown and described herein, it will be obvious to those skilled in the art that such embodiments are provided by way of example only. Numerous variations, changes, and substitutions will now occur to those skilled in the art without departing from the disclosed methods and devices. It should be understood that various alternatives to the embodiments of the methods and devices described herein may be employed in practicing the novel approaches disclosed herein. It is intended that the following claims define the scope of the disclosed methods and devices, and that methods and structures within the scope of these claims and their equivalents be covered thereby.

CLAIMS

WHAT IS CLAIMED IS:

1. A method of tethering a biological entity to a substrate comprising:

a) forming a supported lipid bilayer on a surface of a substrate, wherein the supported lipid bilayer comprises an anchor molecule that comprises or bears a first affinity tag that is present in the lipid bilayer at a concentration greater than or equal to 5 mole percent; and

b) contacting the supported lipid bilayer with a biological entity, wherein the biological entity comprises a nonlinear-active label and a second affinity tag capable of binding to the first affinity tag, thereby tethering the biological entity to the supported lipid bilayer in an oriented fashion.

2. The method of claim 1, wherein the nonlinear-active label is second-harmonic active.

3. The method of claim 1, herein the nonlinear-active label is sum-frequency active.

4. The method of claim 1, further comprising detecting a non-linear optical signal arising from the tethered biological entity.

5. The method of claim 1 or 4, wherein the substrate is fabricated from a material selected from the group consisting of glass, fused-silica, a polymer, or any combination thereof.

6. The method of claim 1 or 4, wherein the first affinity and second affinity tags are Ni-NTA and poly-histidine tags.

7. The method of claim 6, wherein the poly-histidine tag is attached to the N-terminus of a protein.

8. The method of claim 6, wherein the poly-histidine tag is attached to the C-terminus of a protein.

9. The method of claim 6, wherein the poly-histidine tag comprises between 4 and 24 histidine residues.

10. The method of claim 6, wherein the poly-histidine tag comprises 8 histidine residues.

11. The method of claim 6, wherein the poly-histidine tag comprises 6 histidine residues.

12. The method of claim 1 or 4, wherein the first affinity tag comprises Co-CMA and the second affinity tag comprises a poly-histidine tag.

13. The method of claim 1 or 4, wherein the first affinity tag comprises biotin and the second affinity tag comprises streptavidin.

14. The method of claim 1 or 4, wherein the first affinity tag comprises biotin and the second affinity tag comprises avidin.

15. The method of claim 1 or 4, wherein the first affinity tag comprises biotin and the second affinity tag comprises neutravidin.

16. The method of claim 4, wherein the non-linear optical signal is second harmonic light.

17. The method of claim 4, wherein the non-linear optical signal is sum frequency light.

18. The method of claim 4, wherein the non-linear optical signal is difference frequency light.

19. The method of claim 1 or 4, wherein the biological entity is selected from the group consisting of cells, proteins, peptides, receptors, enzymes, antibodies, DNA, RNA, biological molecules, oligonucleotides, small molecules, synthetic molecules, carbohydrates, or any combination thereof.

20. The method of claim 1 or 4, wherein the anchor molecule comprising the first affinity tag is adjusted to a value ranging from 5 mole percent to 100 mole percent of the lipid bilayer.

21. The method of claim 4, wherein the non-linear optical signal detected increases by at least 5x when the concentration of the anchor molecule comprising the first affinity tag is increased by a factor of 2x.

22. The method of claim 4, wherein the non-linear optical signal detected increases by at least 10x when the concentration of the anchor molecule comprising the first affinity tag is increased by a factor of 2x.

23. The method of claim 4, wherein the non-linear optical signal detected increases by at least 20x when the concentration of the anchor molecule comprising the first affinity tag is increased by a factor of 2x.

24. The method of claim 4, wherein the dependence of the non-linear optical signal on the concentration of the anchor molecule comprising the first affinity tag is described by a power law having an exponent greater than 2.

25. The method of claim 1 or 4, further comprising incubating the supported lipid bilayer with the biological entity for about 10 minutes to about 60 minutes.

26. The method of claim 25, wherein the biological entity is present at a concentration of about 0.1 uM to 10 uM.

27. The method of claim 1 or 4, wherein the supported lipid bilayer comprises 1,2-dioleoyl-sn-glycero-3-phosphocholine.

28. The method of claim 1 or 4, wherein the anchor molecule conjugated to the first affinity tag comprises 1,2-dioleoyl-sn-glycero-3-[(N-(5-amino-1-carboxypentyl)iminodiacetic acid)succinyl] (nickel salt).

29. The method of claim 1 or 4, wherein the biological entity is a protein.

30. The method of claim 29, wherein the protein is present at a concentration of less than 2 uM.

31. The method of claim 29, wherein the amount of protein used is less than 500 ng.

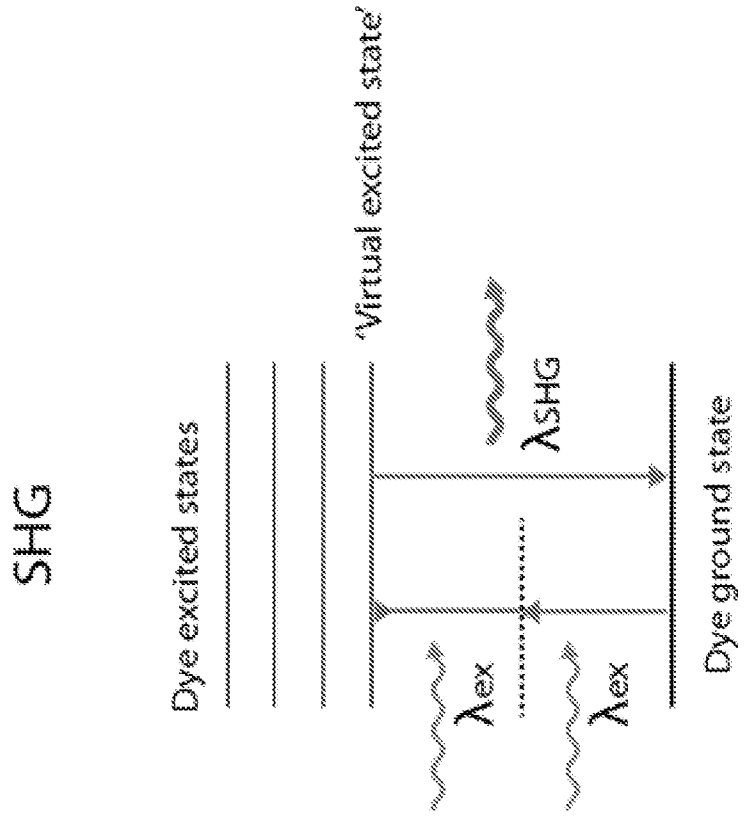
SHG
Dye excited states
'Virtual excited state'
λex
λex
λSHG
Dye ground state

FIG. 1B

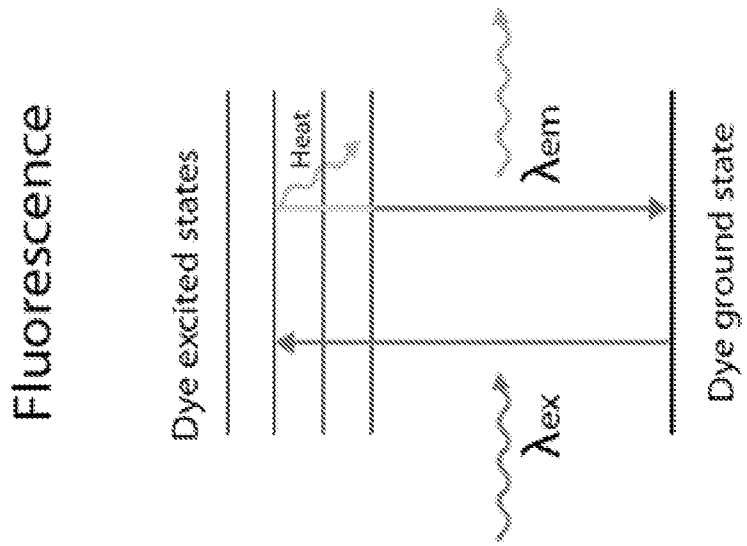
Fluorescence
Dye excited states
Heat
λex
λem
Dye ground state

FIG. 1A

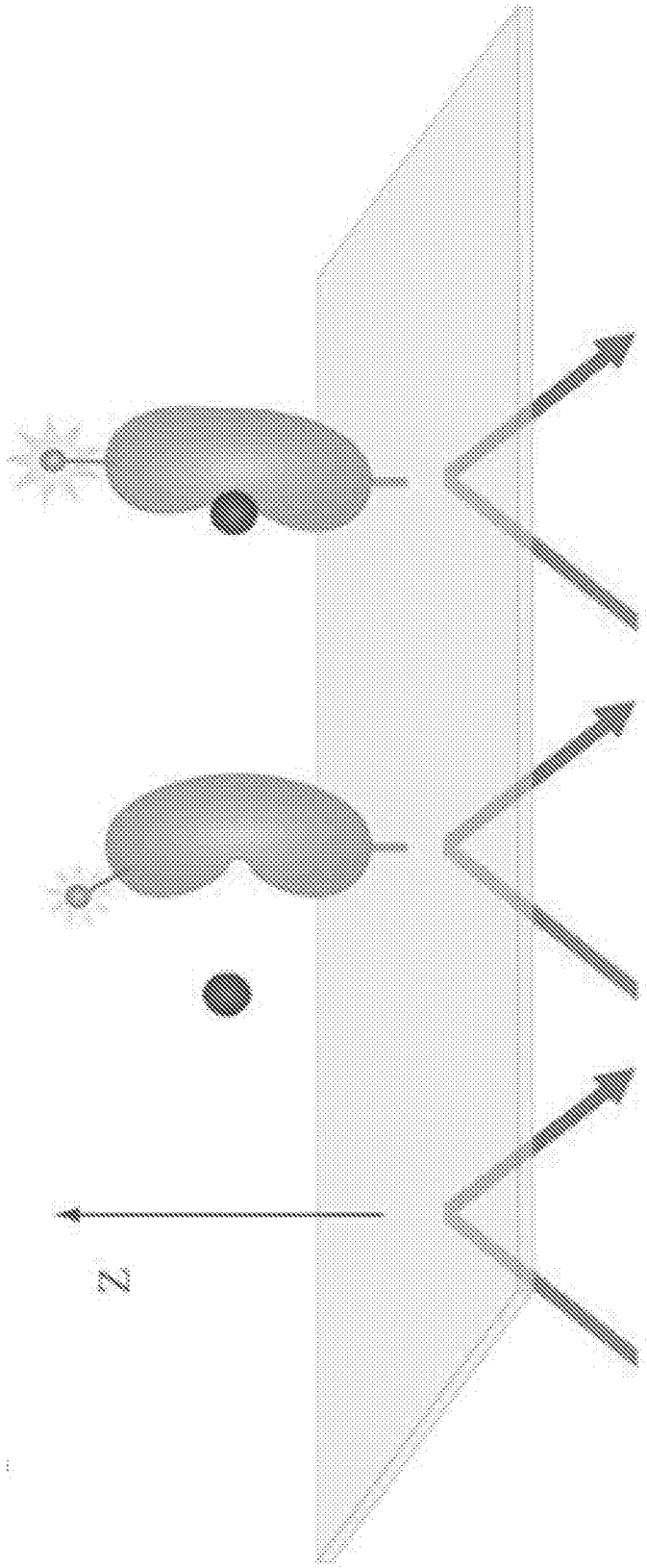

FIG. 2

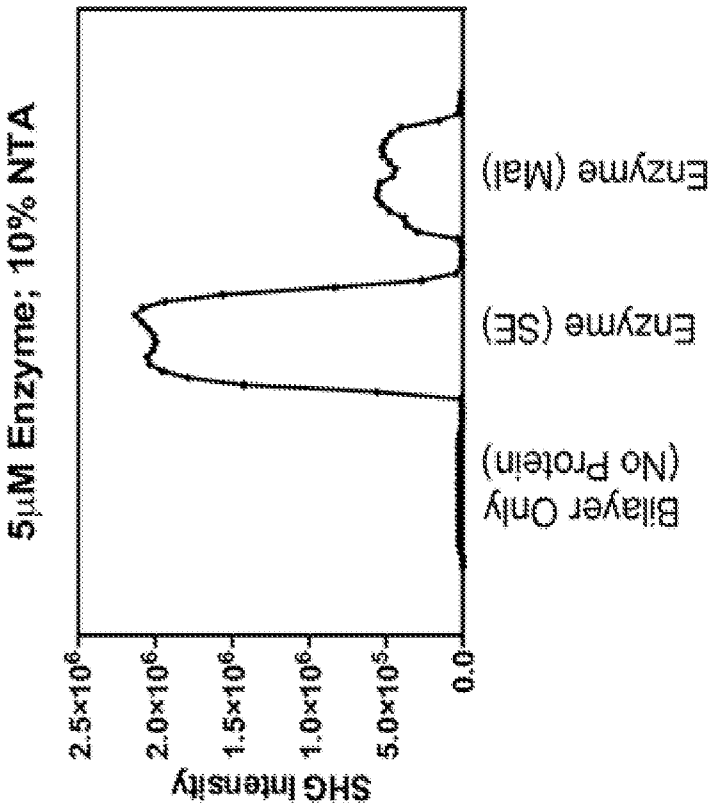
5μM Enzyme; 10% NTA
SHG Intensity
2.5×10^6
2.0×10^6
1.5×10^6
1.0×10^6
5.0×10^5
0.0
Bilayer Only
(No Protein)
Enzyme (SE)
Enzyme (Mal)

FIG. 3

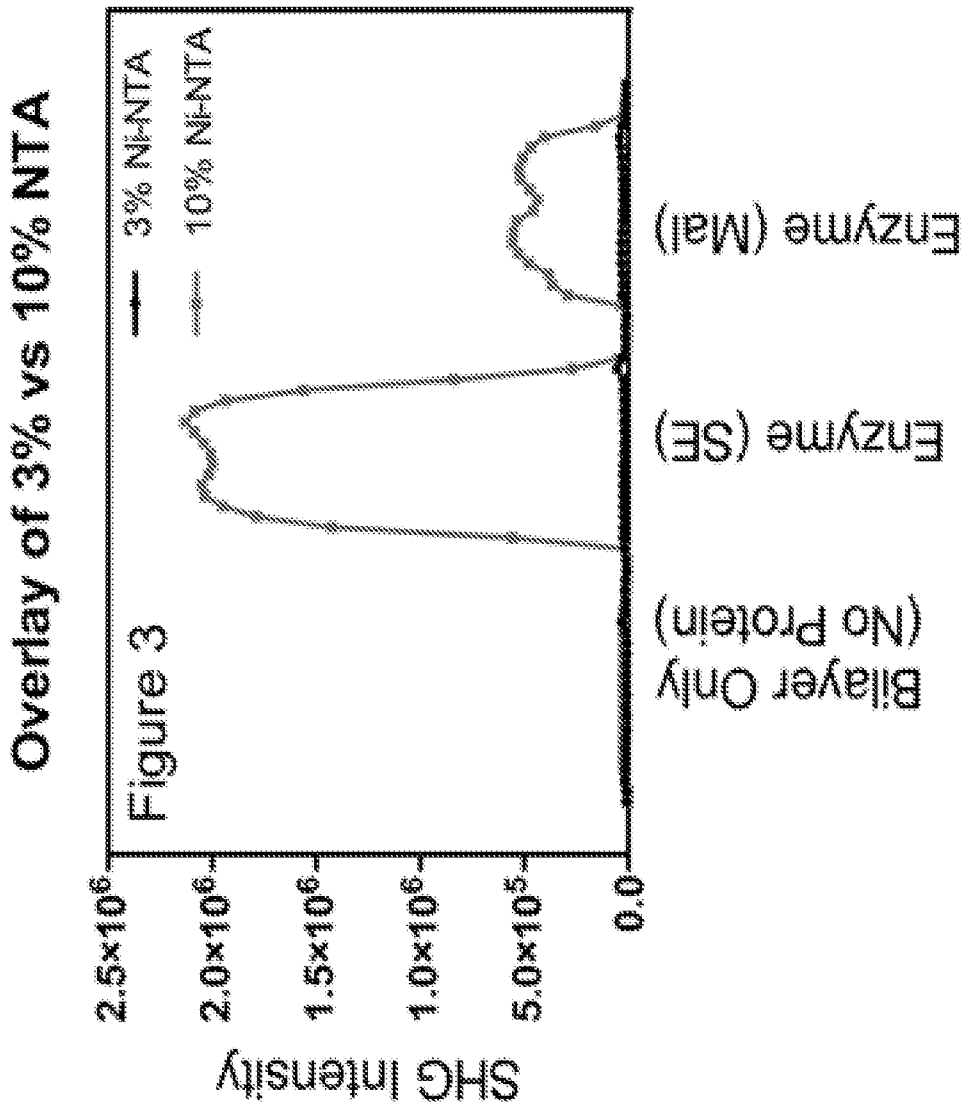
Overlay of 3% vs 10% NTA
3% Ni-NTA
10% Ni-NTA
Figure 3
SHG Intensity
2.5×10^6
2.0×10^6
1.5×10^6
1.0×10^6
5.0×10^5
0.0
Bilayer Only
(No Protein)
Enzyme (SE)
Enzyme (Mal)

FIG. 4

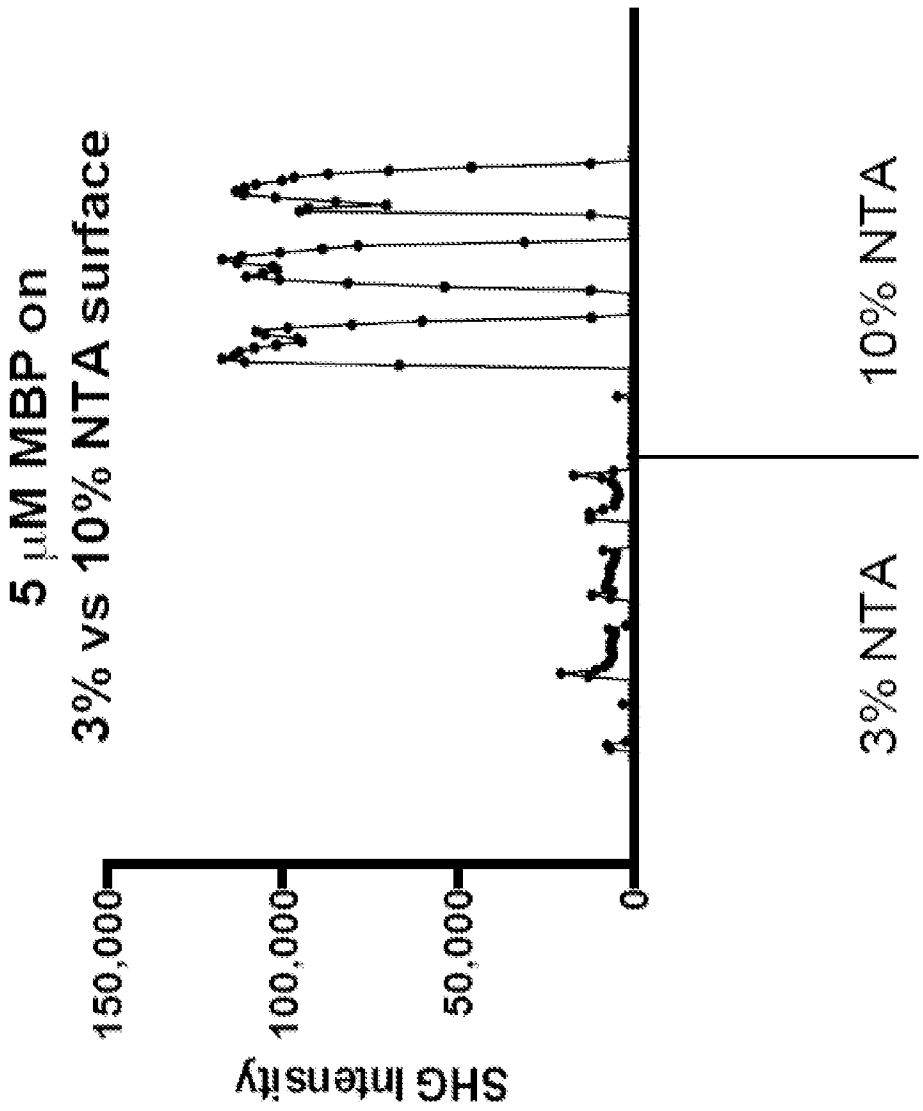
5 μM MBP on
3% vs 10% NTA surface
SHG Intensity
150,000
100,000
50,000
0
3% NTA
10% NTA

FIG. 5

FIG. 6A

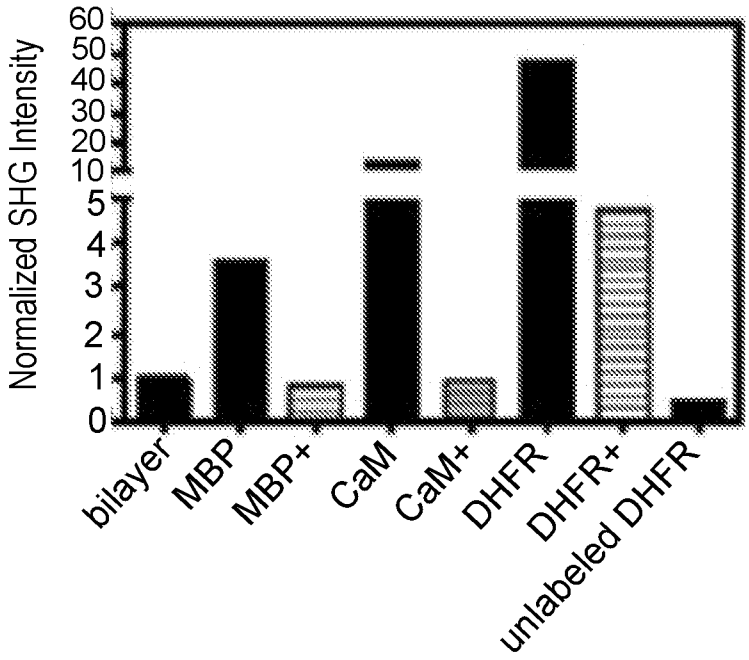

FIG. 6B

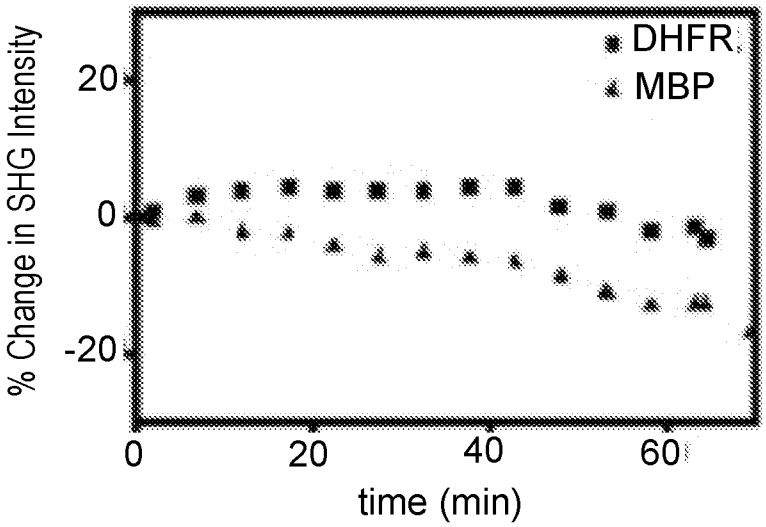

FIG. 6C

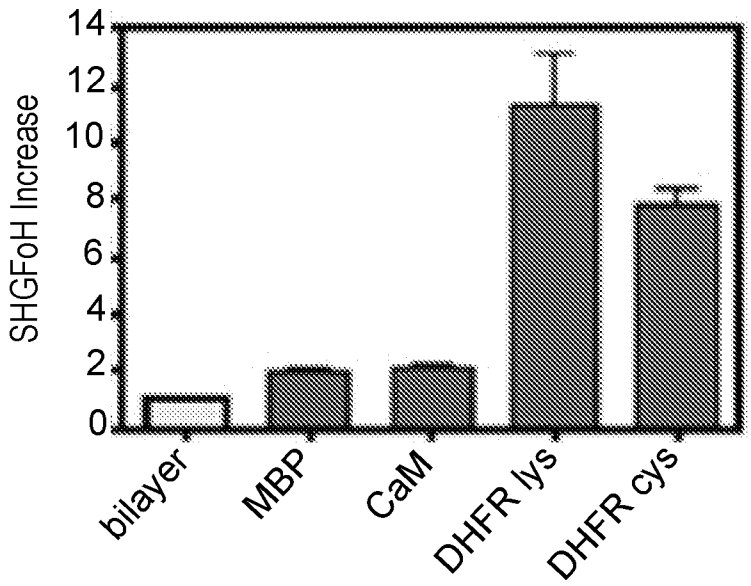

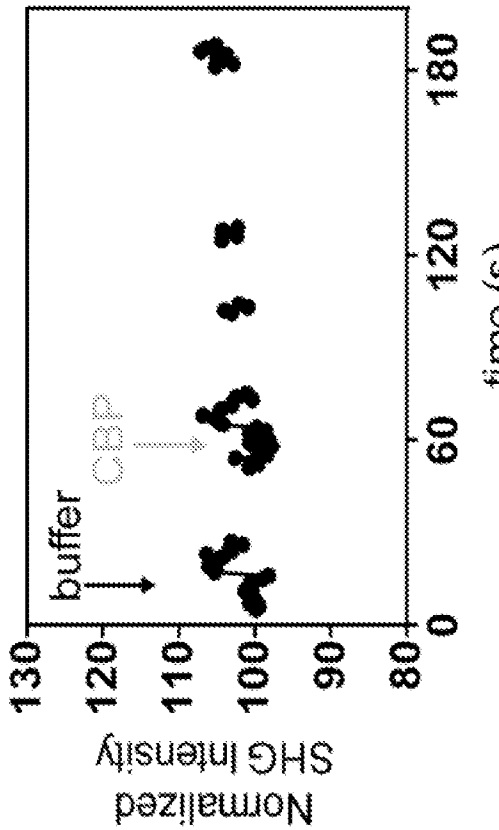

FIG. 7B

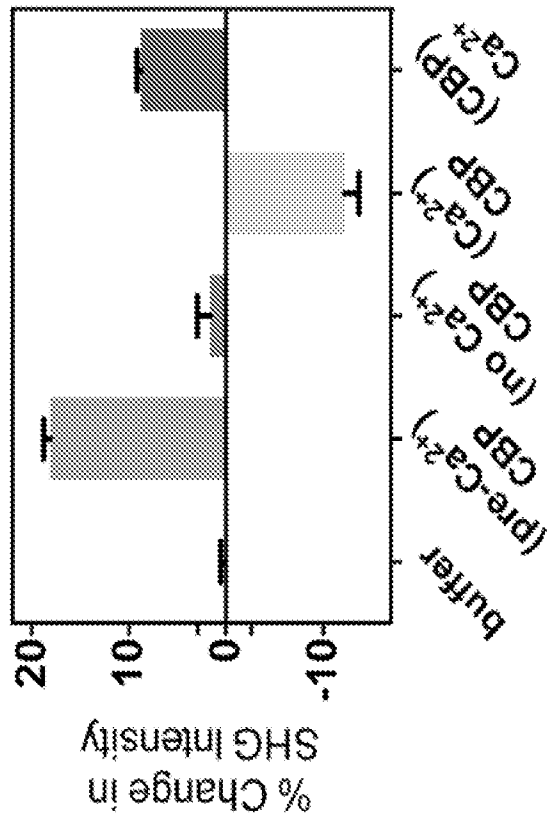

FIG. 7D

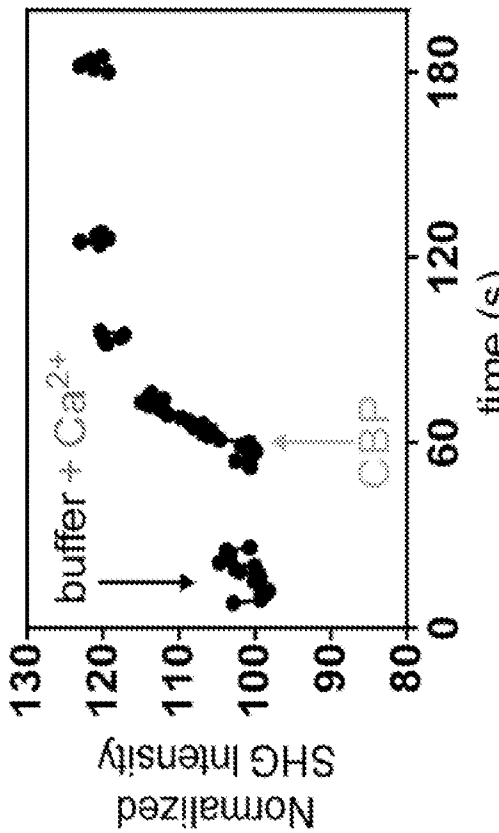

FIG. 7A

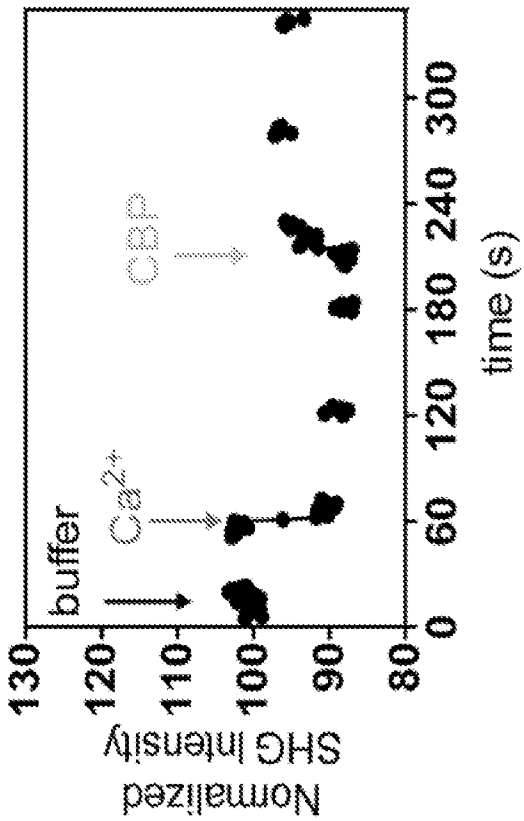

FIG. 7C

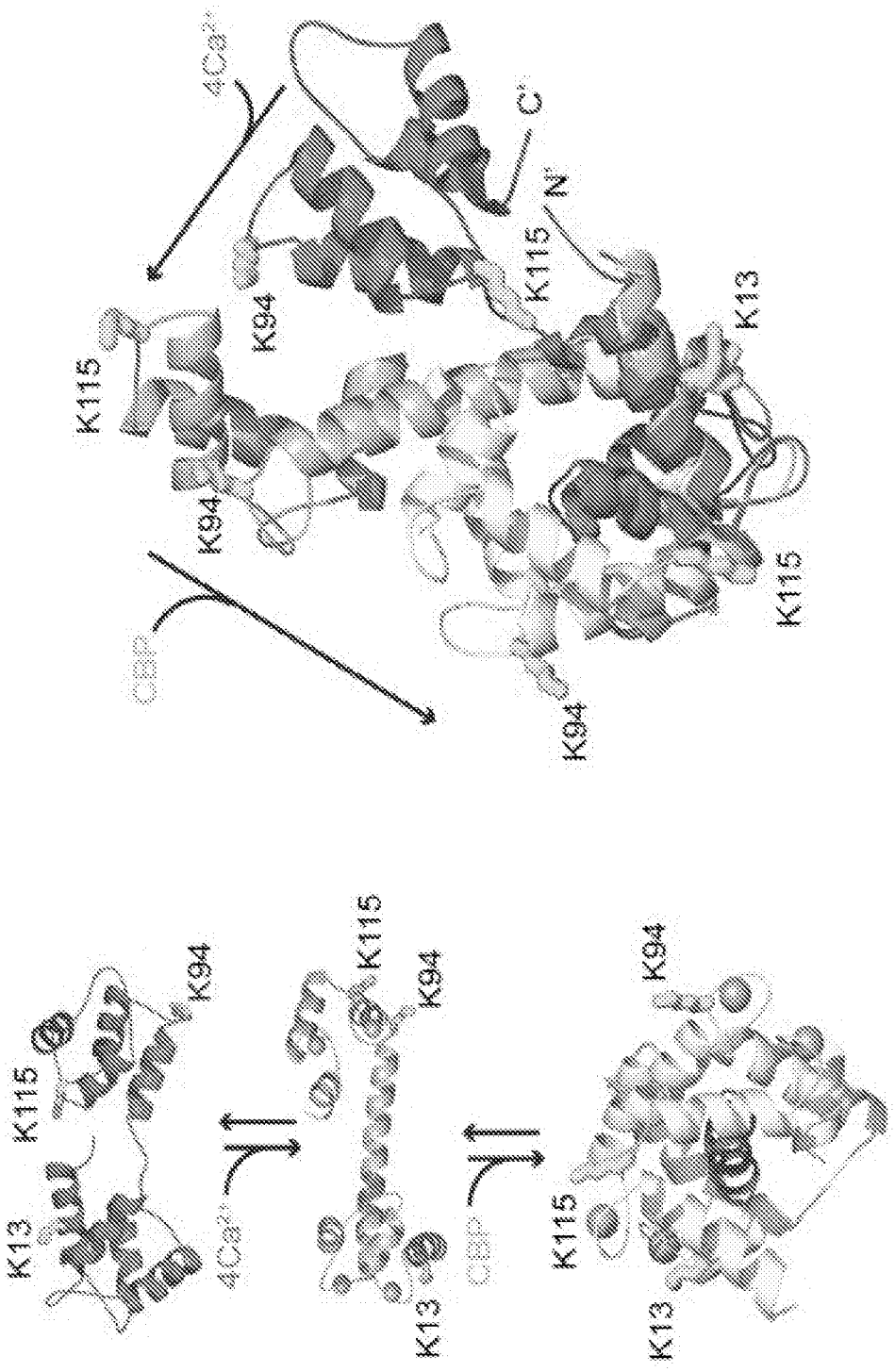
4Ca2+
C'
N'
K115
K94
K13
CBP
K115
K94
K13
K115
K94
4Ca2+
K13
K115
K94
CBP
K115
K94
K13

FIG. 7E

FIG. 8A

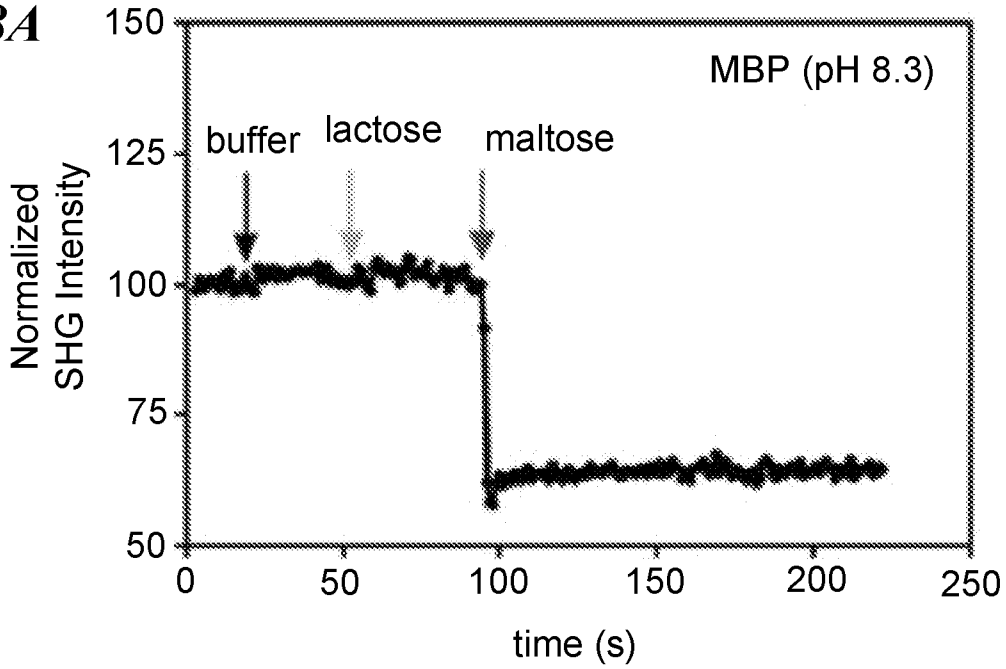
MBP (pH 8.3)
buffer
lactose
maltose
Normalized SHG Intensity
150
125
100
75
50
0
50
100
150
200
250
time (s)

FIG. 8B

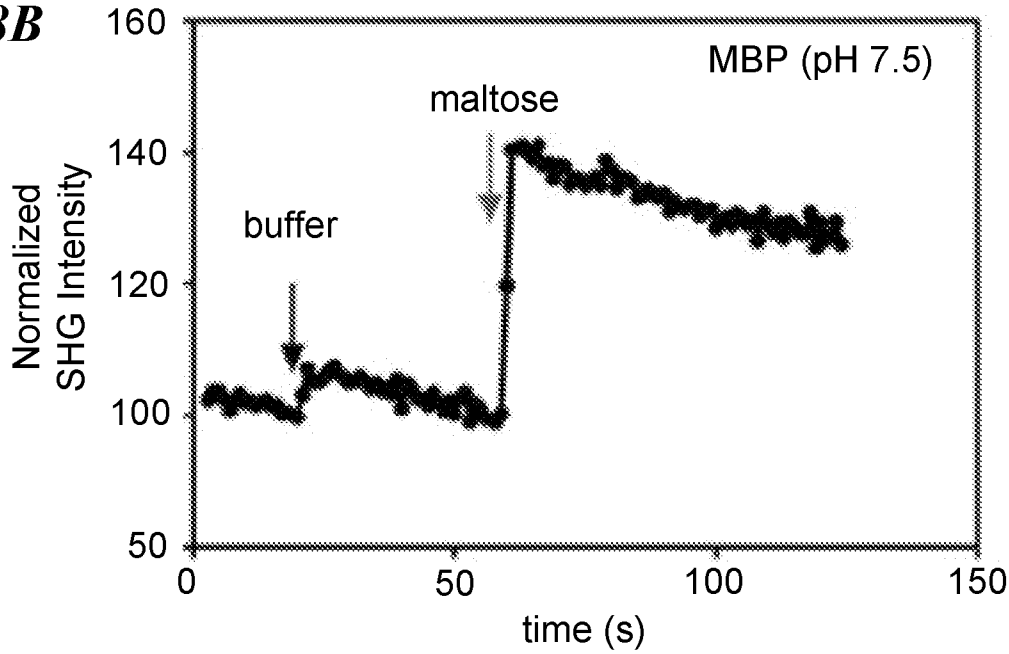
MBP (pH 7.5)
maltose
buffer
Normalized SHG Intensity
160
140
120
100
50
0
50
100
150
time (s)

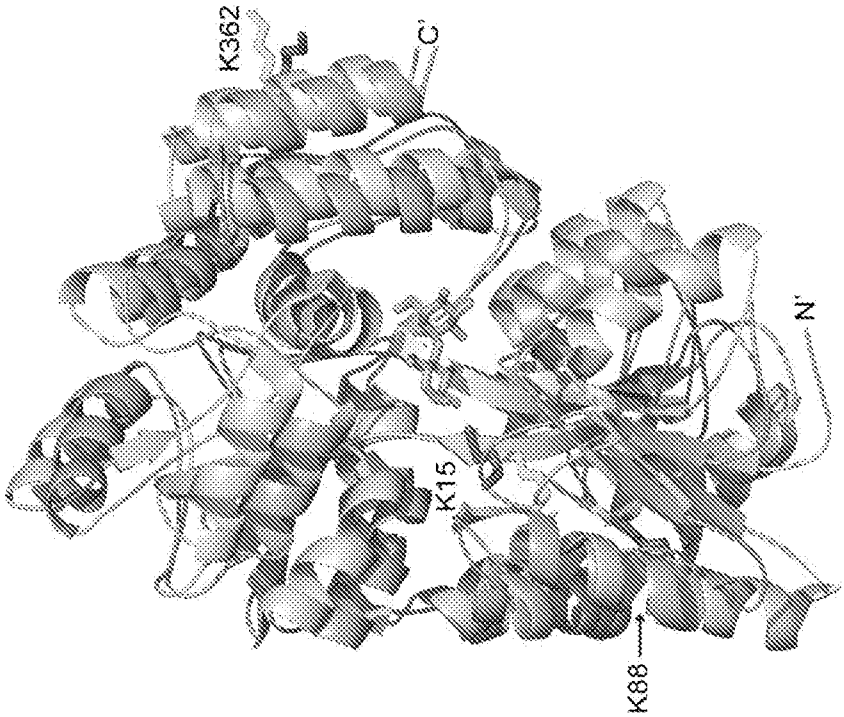
K362
C'
N'
K15
K88

FIG. 8D

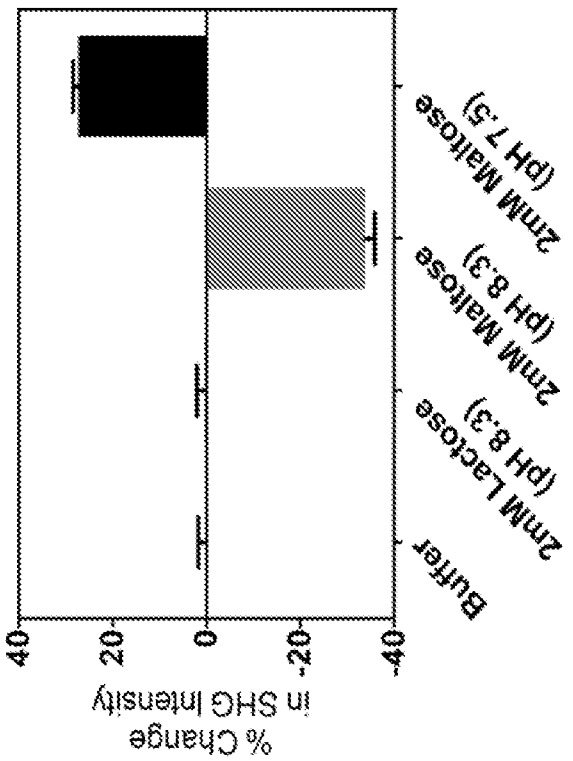
% Change
in SHG Intensity
40
20
0
-20
-40
Buffer
2mM Lactose
(pH 8.3)
2mM Maltose
(pH 8.3)
2mM Maltose
(pH 7.5)

FIG. 8C

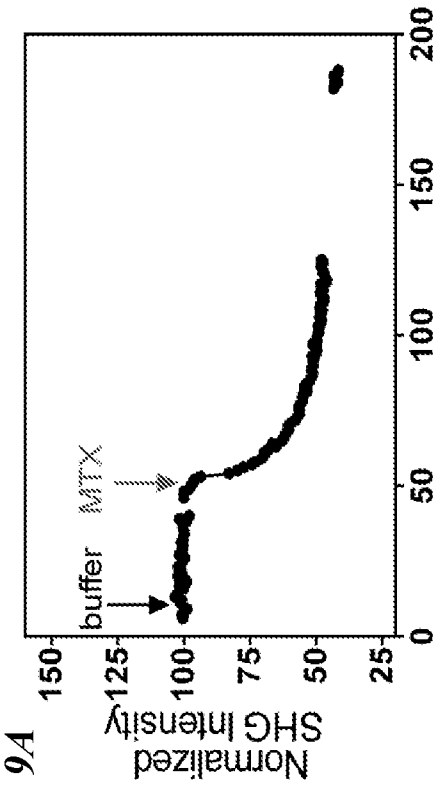
Normalized
SHG Intensity
150
125
100
75
50
25
0
50
100
150
200
time (s)
buffer
MTX

FIG. 9A

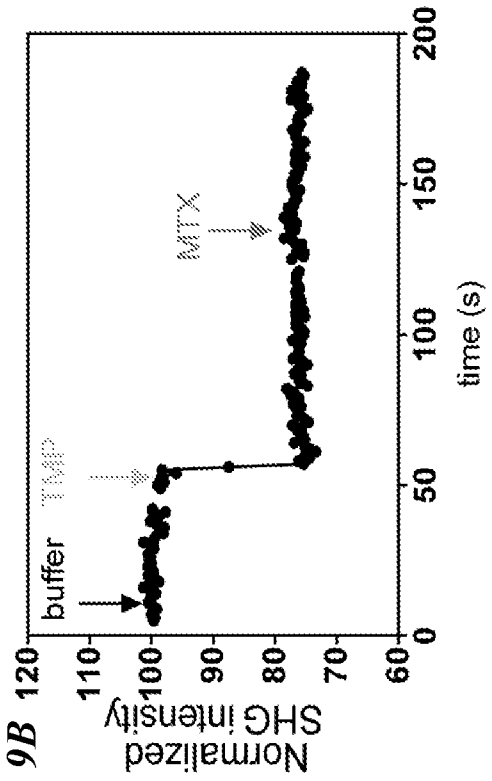
Normalized
SHG intensity
120
110
100
90
80
70
60
0
50
100
150
200
time (s)
buffer
TMP
MTX

FIG. 9B

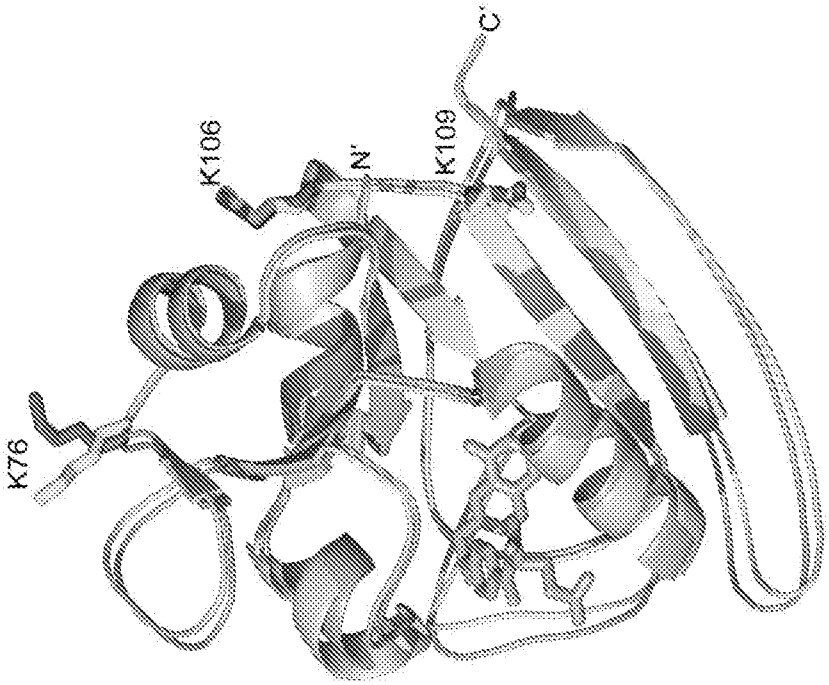
K76
K106
N'
K109
C'

FIG. 9D

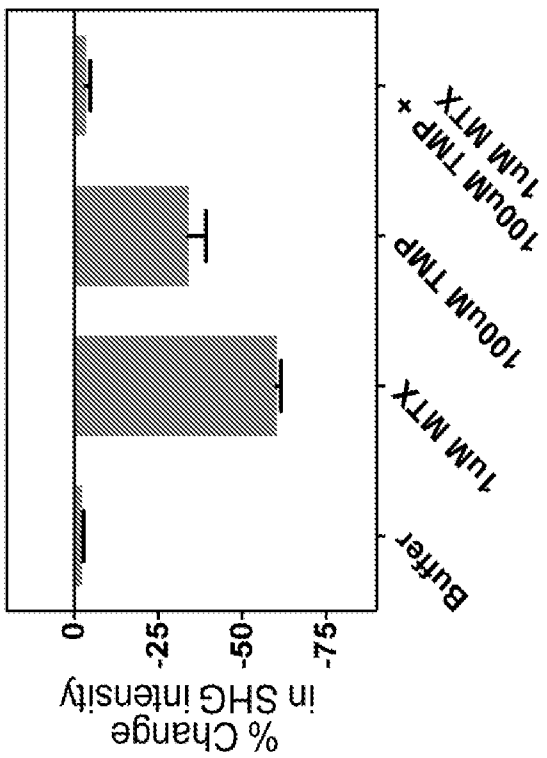
% Change in SHG intensity
0
-25
-50
-75
Buffer
1uM MTX
100uM TMP
100uM TMP + 1uM MTX

FIG. 9C

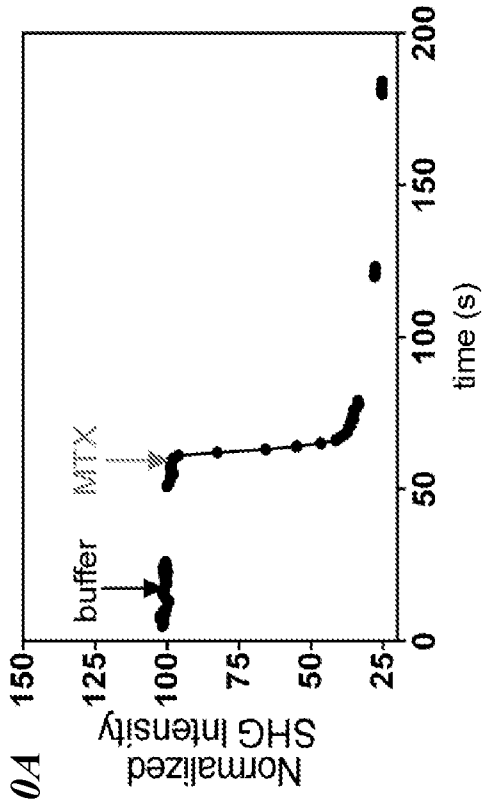

FIG. 10A

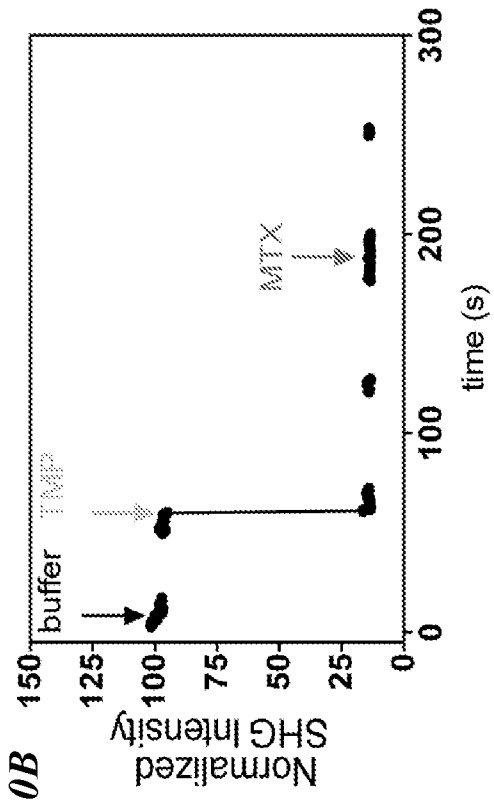

FIG. 10B

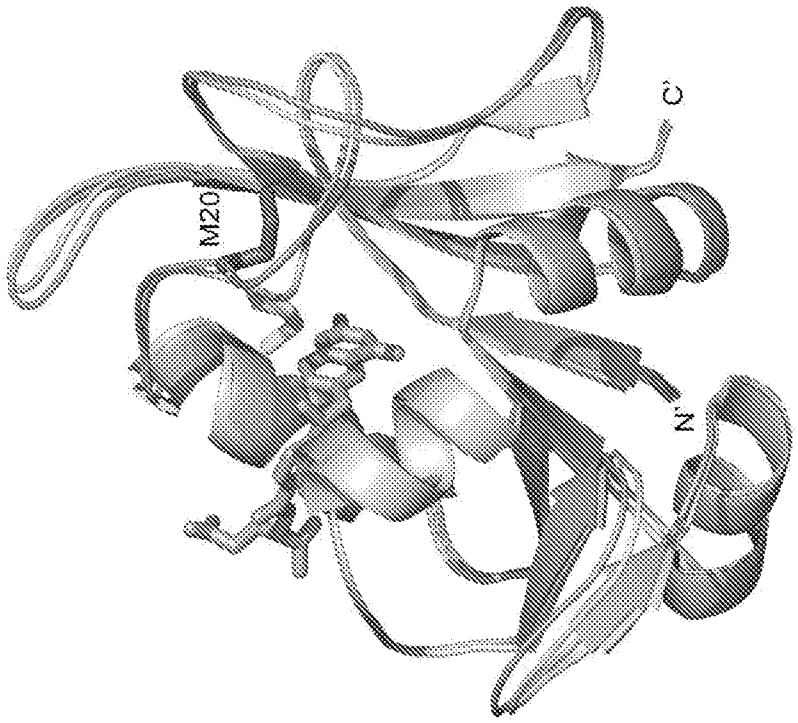

FIG. 10D

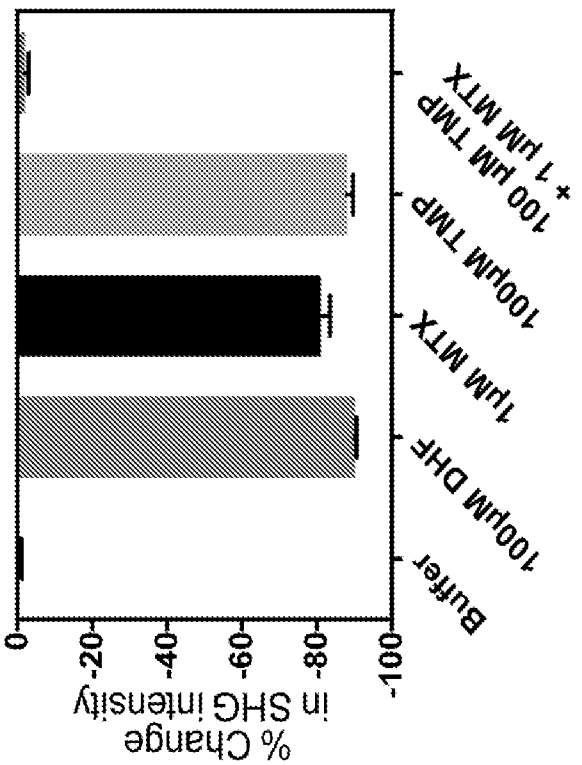

FIG. 10C

FIG. 11A

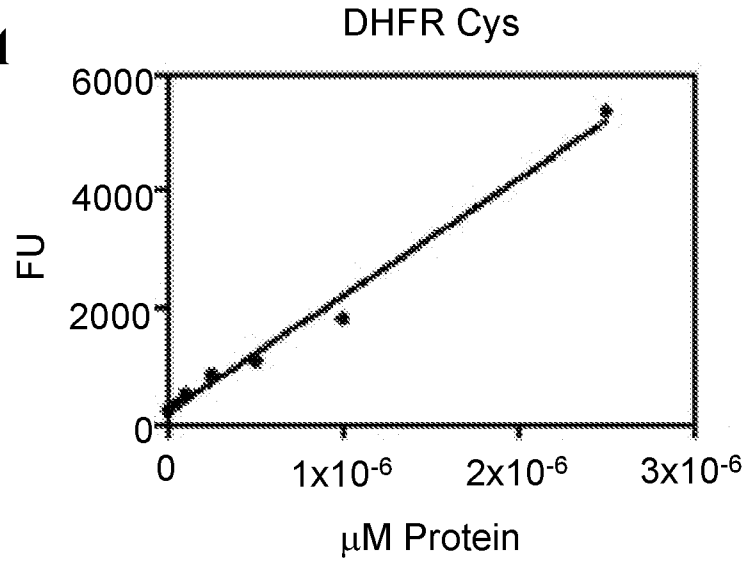

FIG. 11B

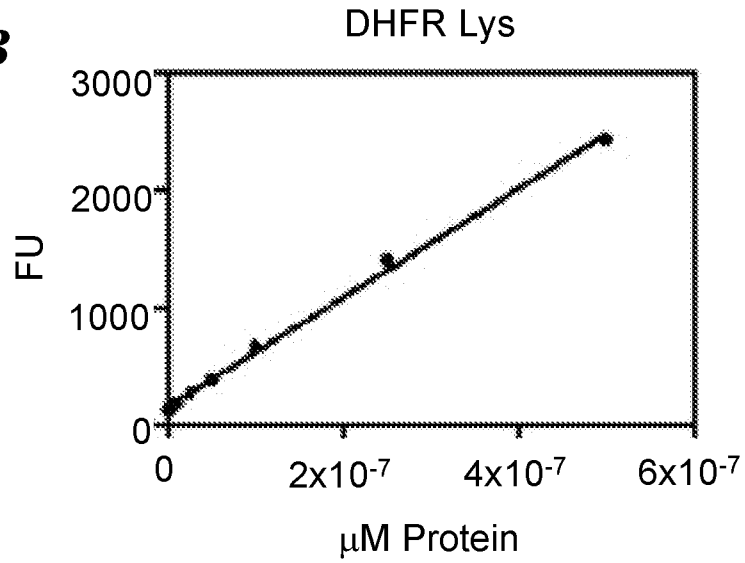

FIG. 11C

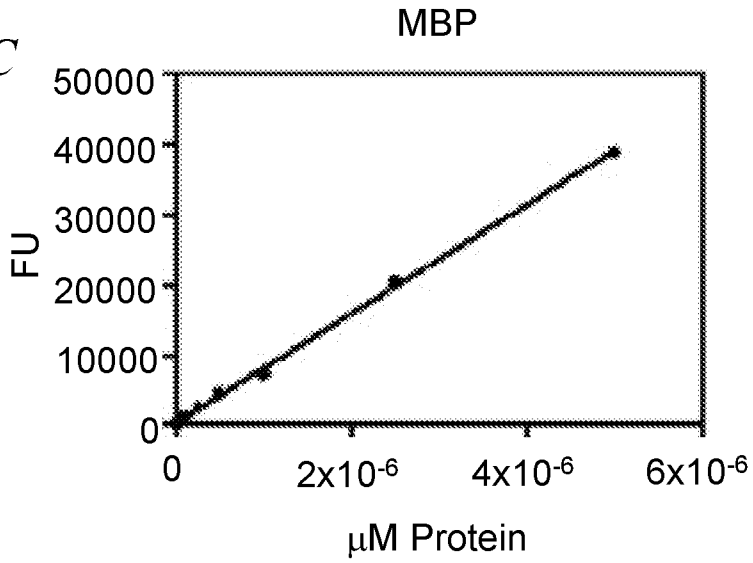

INTERNATIONAL SEARCH REPORT

International application No.
PCT/US 15/67285

A. CLASSIFICATION OF SUBJECT MATTER
IPC(8) - G01N 33/483, G01N 23/20, G01N 33/50, G01N 33/566 (2016.01)
CPC - G01N 33/583, G01N 33/5005, G01N 33/533, G01N 33/54373
According to International Patent Classification (IPC) or to both national classification and IPC

B. FIELDS SEARCHED

Minimum documentation searched (classification system followed by classification symbols)
IPC(8) - G01N 33/483, G01N 23/20, G01N 33/50, G01N 33/566 (2016.01)
CPC - G01N 33/583, G01N 33/5005, G01N 33/533, G01N 33/54373

Documentation searched other than minimum documentation to the extent that such documents are included in the fields searched
UC - 436/164, 436/518, 436/501, 356/300, 435/7.92

Electronic data base consulted during the international search (name of data base and, where practicable, search terms used)
Minesoft Patbase, Google Scholar: tethering biological entity lipid bilayer affinity tag oriented fashion attach protein dnadetection BIODESY, INC.

C. DOCUMENTS CONSIDERED TO BE RELEVANT

Category*	Citation of document, with indication, where appropriate, of the relevant passages	Relevant to claim No.
Y	US 2013/0288271 A1 (Salafsky) 31 October 2013 (31.10.2013) para [0008], [0014], [0024], [0098], [0124], [0138], [0140], [0149], [0157]	1-31
Y	US 2008/0038281 A1 (Altin et al.) 14 February 2008 (14.02.2008) abstract, [0059]	1-31
Y	US 2007/0172947 A1 (Shirwan) 26 July 2007 (26.07.2007) para [0152]	12
Y	WO 2013/115867 A1 (BIODESY) 08 August 2013 (08.08.2013) para [0139]	13, 14
Y	US 2012/0202296 A1 (Eisenthal) 09 August 2012 (09.08.2012) para [0045]	15
Y	US 2003/0148391 A1 (Salafsky) 07 August 2003 (07.08.2003) abstract, para [0433]	18
Y	US 2005/0259249 A1 (Dombeck et al.) 24 November 2005 (24.11.2005) para [0088]	21-23
Y	US 2011/0014612 A1 (Hendricks et al.) 20 January 2011 (20.01.2011) para [0647], [0653], [0654]	24

☐ Further documents are listed in the continuation of Box C. ☐

* Special categories of cited documents:
"A" document defining the general state of the art which is not considered to be of particular relevance
"E" earlier application or patent but published on or after the international filing date
"L" document which may throw doubts on priority claim(s) or which is cited to establish the publication date of another citation or other special reason (as specified)
"O" document referring to an oral disclosure, use, exhibition or other means
"P" document published prior to the international filing date but later than the priority date claimed
"T" later document published after the international filing date or priority date and not in conflict with the application but cited to understand the principle or theory underlying the invention
"X" document of particular relevance; the claimed invention cannot be considered novel or cannot be considered to involve an inventive step when the document is taken alone
"Y" document of particular relevance; the claimed invention cannot be considered to involve an inventive step when the document is combined with one or more other such documents, such combination being obvious to a person skilled in the art
"&" document member of the same patent family

Date of the actual completion of the international search	Date of mailing of the international search report
14 February 2016 (14.02.2016)	03 MAR 2016
Name and mailing address of the ISA/US Mail Stop PCT, Attn: ISA/US, Commissioner for Patents P.O. Box 1450, Alexandria, Virginia 22313-1450 Facsimile No. 571-273-8300	Authorized officer: Lee W. Young PCT Helpdesk: 571-272-4300 PCT OSP: 571-272-7774

Form PCT/ISA/210 (second sheet) (January 2015)